Chapter-2: SUPPORTS – EXPERIMENTAL, RESULTS AND DISCUSSION

Abstract

Preparation of Zirconia-alumina bicomponent supports is studied. Deposition-precipitation is compared with co-precipitation. Three different alumina based substrates, varying in their surface area, hydroxyl content and ease of peptization are evaluated for deposition-precipitation. Effect of pH of precipitation from pH 7 to 10 is studied. The as synthesized samples are characterized for their physico-chemical characteristic. Pro and Cons of the two methods of preparation are determined.

Characterization techniques TGA-MS, CHN and ICP-OES are used for determining the detailed composition of zirconia compounds and their interactions with the substrates. Effect of pH on composition is also determined. FTIR is used to determine chemical nature of zirconia-carbonate species. The composition of as-synthesized supports is determined.

N_2 physisorption is used to determine microstructure (specific surface area, specific pore volume and average pore diameter) and the influence of pH of preparation and substrate on these characteristics. XRD crystallite size and acidity of calcined samples are compared. SEM-EDAX is used to study morphology of select samples.

The above properties are correlated with activity and stability of the supports for the decomposition of MBOH (methyl butanol). Acidity of the supports is determined from selectivity of this reaction.

The results are used for selection of substrate and pH for the preparation of a final set of supports which are used for preparing bifunctional supported metal catalysts (covered in Chapter 3). These in turn are evaluated for i) the transformation of styrene oxide to phenyl acetaldehyde and 2-phenyl ethanol (covered in Chapter 4) and ii) for the hydrodeoxygenation of m-cresol (covered in Chapter 5).

2.1 Introduction

Catalyst supports play an important role in supported metal catalysis. They contribute by way of surface area for dispersion of the active metal phase. Further, supports interact with active metals (metal support interaction - MSI) which influences the reducibility of the active metal, imparts resistance to active metal sintering and in turn influence its activity and stability. Supports enable diffusivity of reactants and products by providing porosity. They also impart thermal stability and mechanical strength in formed catalysts. The supports also have inherent acidity-basicity which is important for reactions requiring bi-functional catalysts. It also influences product selectivity and catalyst stability due to coking. Thus, selection of an appropriate support is important.

Supports reported in literature for the reactions planned in the current work, viz. transformation of styrene oxide and the hydrodeoxygenation (HDO) of m-cresol are reviewed below.

Various support materials such as refractory metal oxides, aluminosilicates (zeolites), amorphous silica-alumina and activated carbons are reported. Noble metals such as Pt or Pd and transition metals such as Co, Ni and Cu are reported as the active metals. A survey of literature indicates that use of alumina, silica, titania, MgO, hydrotalcites, silica-zirconia, silica-alumina, zeolites [1][2][3][4][5][6][7][8] and activated carbon[9] is reported for transformation of styrene oxide (SO) to phenylacetaldehyde (PAA) and 2-phenylethanol (2-PEA)[1][10]. This is discussed in detail in Chapter 4[9]. Amongst these, activated carbon is reported for hydrogenation of styrene oxide to 2-phenylethanol[9]. However, removal of coke deposits for regeneration is expected to pose a problem in the case of activated carbons. On the other hand, refractory oxides can be easily regenerated by thermal oxidation of coke.

Amongst the refractory oxides basic support MgO is reported to be suitable for reductive cleavage of SO to 2-PEA[11]. However according to[11] Bergada, MgO provides good performance provided its basicity is masked by the active metal, otherwise deactivation occurs due to condensation reactions which foul the catalyst. Acidic supports such as silica-alumina and zeolites[6][2] are reported to catalyze the isomerization of styrene oxide to phenylacetaldehyde. These are also reported for hydrogenation of SO to 2-phenylethanol. Between the two, zeolites are microporous and have strong Brönsted acidity. Which is not desirable from perspective of

diffusivity and fouling due to coke formation. Thus both acidic and basic supports have their own pros and cons for this reaction. Both alumina and zirconia present amphoteric properties. They have good Lewis acidity. In addition, alumina has Brönsted acidity. A combination of zirconia-alumina is not studied / reported for transformation of styrene oxide to PAA or 2-PEA. Such a combination would make for an interesting study as a support.

The hydrodeoxygenation of phenol and its derivatives has been widely studied. Various refractory oxides such as alumina, silica, titania, ceria, zirconia, and bi-component supports such as silica-alumina, silica-zirconia, ceria-zirconia are reported / reviewed in literature for this[12][13][14] reaction. γ-Alumina is reported to degenerate due to rehydration to boehmite by water which is a reaction product [15]. Silica has poor acidity and is hence disadvantaged for formation of aromatics. Zirconia is reported to exhibit resistance to coking, however it suffers from low surface area. Zirconia-alumina materials are known for their hydrothermal stability and are widely used in conditions where moisture is present (prosthetics)[16] and automotive exhaust catalysts[17]. Thus bi-component zirconia-alumina would be an interesting candidate as a support for study.

The combination of support, active metal and reaction conditions influences product selectivity[18][19][20]. A multitude of products ranging from cyclohexanone, cyclohexanol, BTX (Benzene-Toluene-Xylene), methane, cyclohexane, methylcyclohexane, xylenol, phenol etc. are reported for HDO of m-cresol.

However, studies in literature are fragmented and differ in one or more of method of preparation, support, active metal, reaction conditions etc. making it difficult to compare and understand the effect of individual active metals. Use of zirconia-alumina bi-component support is not reported for both the transformation of styrene oxide or the hydrodeoxygenation of m-cresol.

Deposition-precipitation is a simple and useful technique for preparation of supports/catalysts, wherein one component is precipitated from solution in the presence of a solid substrate for preparing bicomponent materials[21][22][23][24]. The solid substrate is a material with high specific surface area and pore volume. It lends these properties for good dispersion of the second (precipitated) component thus improving the overall surface area of the bicomponent product. It is useful when the component which is precipitated tends to have low surface area when it is precipitated independently (such as zirconia in the present study). N.M. Deraz[21] has

reviewed the method of deposition-precipitation with adsorption based methods. He has provided references citing that this method is used when adsorption capacity of a substrate for the active component is a limiting factor[22]. C. Perego and P. Villa[23] have covered the general procedure of this method in their review article. L.S. Roselin et al. [24] have compared bimetallic Au-Ru/Fe_2O_3 catalysts prepared by deposition-precipitation with those prepared by co-precipitation. They report that the catalysts prepared by the former method have superior specific surface area and better activity than those prepared by the latter method. Thus, deposition-precipitation may be a useful method of catalyst preparation in the scenario where the active component in itself or a co-precipitated bicomponent material tends to have a low surface area and or porosity.

In contrast coprecipitation comprises simultaneous precipitation of two components from their solutions at a constant pH or to a final pH (Strike precipitation).

In the present work bi-component supports of two amphoteric metal oxides, alumina and zirconia are studied. The support has commonality for both the transformation of SO to PAA and 2-PEA as well as HDO of m-cresol (substituted phenolics).

These supports were prepared either by precipitation (neat zirconia support) or by co-precipitation or deposition-precipitation (bi-component zirconia-alumina supports) to study the effect of method of preparation. Supports were also prepared by physically mixing powder of substrate with freshly precipitated zirconia as a control to understand the effect of deposition-precipitation. Samples of neat zirconia and neat γ-Al_2O_3 were also part of the study.

Based on the results of this study a set of bi-component supports with zirconia:alumina varying from 0:1 to 1:0 were prepared. These were used for preparation of supported metal catalysts which in turn were characterized and evaluated for the transformation of styrene oxide and HDO of m-cresol. These studies are reported in chapters 3, 4 and 5 respectively.

2.2 Experimental

Method of preparation is an important factor which affects properties of final support/catalyst. In order to understand effect of method of preparation bi-component zirconia alumina supports were prepared by deposition-precipitation and also by co-precipitation method. To understand the interaction between zirconia and alumina during deposition-precipitation a

series was prepared by physical mixing of powder of gamma alumina with freshly precipitated zirconia. Effect of pH was studied for the different methods of preparation.

Nature and properties of starting materials influence properties of the final catalyst. Hence, in the initial screening study different precursors of alumina were used as substrates to prepare bi-component zirconia alumina supports by deposition-precipitation method. The composition of supports was maintained at 1:1 ZrO_2:Al_2O_3 mole basis. Apart from γ-alumina (GA), Aluminum trihydrate (ATH) and aluminum monohydrate (AM) were used as sources of alumina substrates for deposition-precipitation. ATH is also referred to as aluminum trihydrate. These substrates differ significantly in their specific surface areas, their degree of hydroxylation, acidity and peptization behavior. Hydrolysis and condensation through olation or oxolation take place during (co)-precipitation. In deposition-precipitation some condensation could occur through reaction between precipitated zirconia and the surface hydroxyls of the substrate.

Samples prepared using co-precipitation method are designated as CP series while samples prepared by physical mixing are designated PHY series. Nomenclature used for the samples prepared by deposition-precipitation was name of the substrate (AT, AM or GA) representing a given series followed by the value of pH of precipitation. Example GA-7 means support prepared by deposition-precipitation using γ-Al_2O_3 as substrate and precipitation of zirconia at pH 7.

Effect of pH of precipitation on zirconia has been studied by many researchers [25][26][27][28]. These studies report precipitation of zirconia at various pH ranging from 4-10. They also state the effect of pH on phase evolution of zirconia[29][28][30]. The effect on textural properties is been reported. However, this has not been linked to the composition of the as synthesized supports in these studies. In order to understand the effect of pH on different physico-chemical properties all the supports were prepared at four levels of pH viz. 7, 8, 9 and 10. The series prepared by deposition-precipitation and using aluminum trihydrate support is designated as AT series. Similarly the series prepared using aluminum monohydrate is designated as AM series, the series prepared using γ-alumina is designated as GA series. Neat zirconia was also precipitated in order to compare with bi-component supports. The composition of as synthesized GA and ZrO_2 series of supports was elucidated through characterization using TGA-MS and CHN analysis. Type of metal-carbonate was elucidated by FTIR.

Finally, a set of bi-component supports with varying zirconia to alumina (ZrO_2:Al_2O_3) molar ratio were prepared by deposition-precipitation at pH 9 using γ-alumina and zirconium nitrate solution. Total 5 supports were prepared with ZrO_2:Al_2O_3 molar ratio of 1:0, 0.75:0.25, 0.5:0.5, 0.25:0.75 and 0:1. These formed the carriers which were used for preparation of the supported metal catalysts which were then used for the transformation of Styrene oxide (chapter 4) and for HDO of m-cresol (chapter 5). Details of preparation and characterization of this set of supports and the supported metal catalysts is covered in Chapter 3.

2.2.1 Materials

An aqueous solution of zirconium nitrate (12.4 wt% as Zr) laboratory grade, Aluminum nitrate of purity 99.9 wt% and sodium carbonate of purity 99.9% were sourced from M/s S.D. fine chemicals.

Aluminum trihydrate (ATH) with purity 99.5 wt% was obtained from M/s HINDALCO. Aluminum monohydrate with purity 99.9 wt% was sourced from Sud-chemie India Pvt. Ltd. γ-alumina was obtained by calcining aluminum monohydrate in air at 550°C for 8h.

2.2.2 Method

2.2.2.1 Preparation of Bi-component zirconia-alumina support by Deposition-precipitation

Figure 2.1 shows a flow chart of the method of preparation of neat zirconia by strike precipitation and bicomponent zirconia-alumina supports by deposition precipitation.

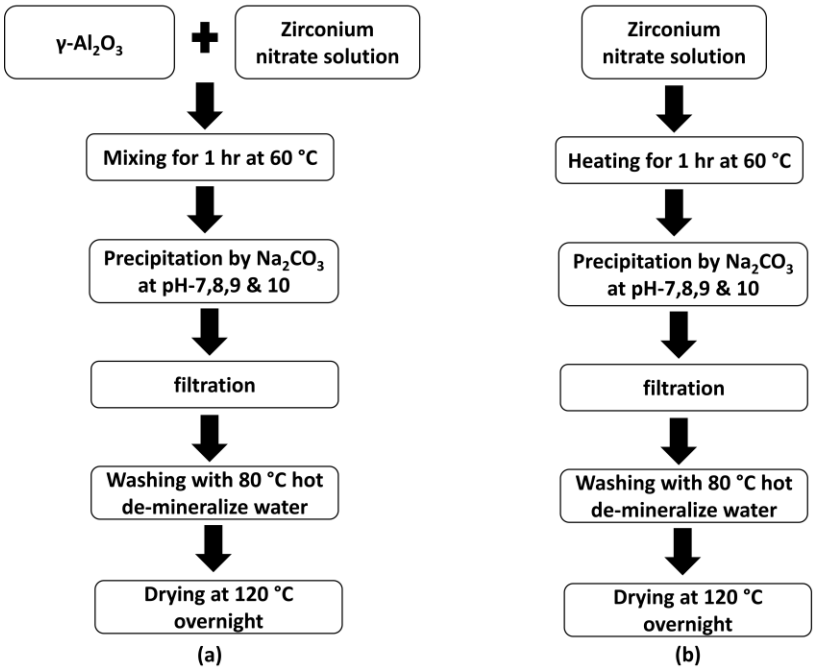

Figure 2. 1: Flowchart for (a) deposition-precipitation of zirconia-alumina supports (b) precipitation of neat zirconia

Equal weight of demineralized water was added to the aqueous solution of zirconium nitrate. The solution was agitated with a mechanical stirrer in a glass beaker. Appropriate quantity of γ-alumina (82.2 g in this specific case), with an average particle size 'd50' 8 μm was added to the above solution under agitation. The 'd50' was determined using a Malvern make model Mastersizer 3000 laser diffraction instrument. Stirring was continued for further 10 min at room temperature, during which the mixture was heated to 60°C on a hot-plate and held at that condition for 1h. 2.5 M Na_2CO_3(aq) was fed to the slurry using a Watson Marlow make model QDos30 peristaltic pump till a stable pH (7 in this specific case) was achieved. The pH was monitored with a Mettler-Toledo make model Easysense31 pH meter fitted with a glass electrode.

Upon completion of precipitation the precipitate was filtered and washed thrice with hot demineralized water (80°C) to remove sodium nitrate (product of precipitation) and also excess sodium carbonate precipitant. The sample was dried in a hot air convection oven at 120°C for 12 hours and ground mildly with an agate mortar and pestle into powder form. This sample, which is precipitated at pH 7 is referred to as GA-7 in the subsequent part of this study. Three more samples

labelled GA-8, GA-9 and GA-10 were prepared by the same procedure as described above, with the exception that the final pH of precipitation was maintained at 8, 9 and 10 respectively.

Samples using Aluminum trihydrate as source of alumina (AT-7, AT-8, AT-9 and AT-10), and using aluminum monohydrate as source of alumina (AM-7, AM-8, AM-9 and AM-10) were prepared by deposition-precipitation as described above. Particle size of ATH was d50 18μ and that of AM was d50 9 μm.

Samples of neat zirconia, ZrO_2-7, ZrO_2-8, ZrO_2-9 and ZrO_2-10 were prepared by strike precipitation at final pH 7, 8, 9 and 10. The alumina component was excluded in these samples.

Physical Mixing of precipitates as control experiment was also performed. A series of control samples GA-PHY-7, GA-PHY-8, GA-PHY-9 and GA-PHY-10 (where the numerals stand for the final pH of preparation) were prepared wherein the zirconium component was first precipitated at target pH as described earlier. The powder of carrier (γ-Al_2O_3) was then added to this precipitate under agitation. The sample was then filtered, washed and dried as per the procedure described above. This amounted to preparation in the form of a physical mixture.

Samples of aluminum trihydrate AT(S), aluminum monohydrate AM(S) and γ-alumina GA(S) which constituted the substrates in deposition-precipitation were also studied for comparison.

The samples and their method of preparation is listed in Table 2.1.

Sr	Nomenclature	Carrier	Final pH of preparation	Route of preparation
1	GA-7	γ-Al_2O_3	7	Deposition-precipitation
2	GA-8	γ-Al_2O_3	8	Deposition-precipitation
3	GA-9	γ-Al_2O_3	9	Deposition-precipitation
4	GA-10	γ-Al_2O_3	10	Deposition-precipitation
5	ZrO_2-7	None (monocomponent precipitated Zirconia)	7	Precipitation
6	ZrO_2-8	None (monocomponent precipitated Zirconia)	8	Precipitation
7	ZrO_2-9	None (monocomponent precipitated Zirconia)	9	Precipitation
8	ZrO_2-10	None (monocomponent precipitated Zirconia)	10	Precipitation
9	AT-7	Aluminum trihydrate	7	Deposition-precipitation
10	AT-8	Aluminum trihydrate	8	Deposition-precipitation
11	AT-9	Aluminum trihydrate	9	Deposition-precipitation
12	AT-10	Aluminum trihydrate	10	Deposition-precipitation
13	AM-7	Aluminum Monohydrate	7	Deposition-precipitation
14	AM-8	Aluminum Monohydrate	8	Deposition-precipitation
15	AM-9	Aluminum Monohydrate	9	Deposition-precipitation
16	AM-10	Aluminum Monohydrate	10	Deposition-precipitation
17	CP-7	Not applicable	7	Co-precipitation
18	CP-8	Not applicable	8	Co-precipitation
19	CP-9	Not applicable	9	Co-precipitation
20	CP-10	Not applicable	10	Co-precipitation
21	GA-PHY-7	γ-Al_2O_3	7	Physical blending of precipitate
22	GA-PHY-8	γ-Al_2O_3	8	Physical blending of precipitate
23	GA-PHY-9	γ-Al_2O_3	9	Physical blending of precipitate
24	GA-PHY-10	γ-Al_2O_3	10	Physical blending of precipitate
25	AT(S)	Aluminum trihydrate	-	Substrate / Carrier
26	AM(S)	Aluminum monohydrate	-	Substrate / Carrier
27	GA(S)	Gamma-Al_2O_3	-	Substrate / Carrier

Table 2. 1: Samples prepared for the study

2.2.2.2 Preparation of bi-component zirconia alumina supports by Co-precipitation (CP)

Figure 2.2 shows a flow chart of the method of preparation of bicomponent zirconia-alumina supports by co-precipitation.

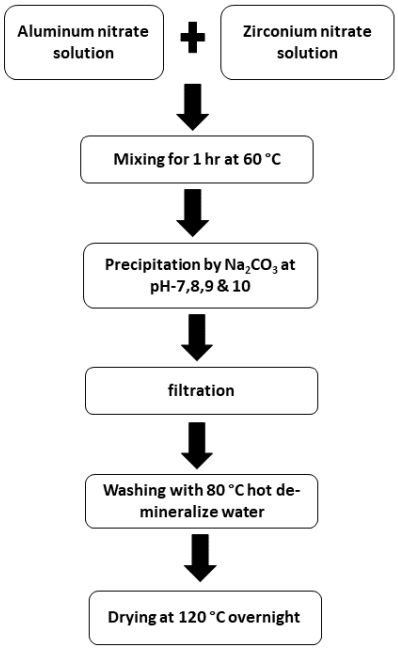

Figure 2. 2: Flowchart of preparation of bicomponent zirconia-alumina supports by co-precipitation method

Solutions of zirconium nitrate (LR grade) of strength 12.4% w/w (as Zr) and of aluminum nitrate (LR grade) of strength 7.5% w/w were used as sources of zirconia and alumina. 368 ml distilled water was taken in a glass beaker to which required quantities of zirconium nitrate and aluminum nitrate solutions (to obtain ZrO_2:Al_2O_3 molar ratio 1) were added under mechanical agitation at 60°C. A solution of sodium carbonate (2.5 M strength) was metered to the above mixture using a Watson-Marlow peristaltic pump till the pH stabilized at a final value of 7. A Mettler-Toledo make Easysense31 model pH meter with a glass electrode was used to measure pH continuously. The precipitate was filtered and washed with hot demineralized water (80 °C) to wash out sodium nitrate and excess sodium carbonate. The sample was dried in a hot air convection oven at 120°C for 12h and ground mildly in an agate mortar and pestle into powder form. This sample is referred to as CP-7. Three more samples were prepared by the same method with the difference that the final pH of precipitation was 8, 9 & 10 respectively. These samples are referred to as CP-8, CP-9 and CP-10.

2.3 Characterization

All the samples were characterized by ICP, powder XRD, N_2 physisorption (for surface area and pore volume), acidity and Thermogravimetry analysis, while GA-series, ZrO_2 series and GA-PHY series were subjected to additional characterization such as CHN, TGA-MS, FTIR, SEM and SEM-EDAX as appropriate.

A Bruker make D8 FOCUS model X-ray diffractometer was used for determining crystallographic phase of the solid samples. The samples were scanned at a scan rate of 2° per min rate with a step size of 0.02 step/s in the 2Θ range of 5 to 80° with a Cu Kα source, wavelength 1.5406 Å

BET specific surface area and pore volume were determined by N2 physisorption with a Quantachrome make QUADRASORB SI IV model instrument. The samples were degassed at 300 °C for a duration of 3 h in a 'Flovac' degasser under vacuum before subjecting them to measurement.

Thermogravimetric studies of all the as-synthesized samples were carried out using a DSC-TG instrument from TA instruments, model Q800 DSC-TG. The sample was charged to platinum boat and heated from ambient temp to 1000 °C at a ramp rate of 10°C/ min. A sweep of air (100 ml/min) was maintained during the measurement. The DSC-TG was coupled to a MKS make Cirrus quadrupole mass spectrometer to identify the gases evolved during the experiment (Evolved gas analysis).

Chemical composition of the supports was determined by ICP OES with a Thermoscientific make, model iCAP 6000 series instrument. The samples were digested in aqua regia and diluted appropriately for measurement.

Sodium content of the supports was determined using an AIMIL Ltd. make model Fotoflame Flame photometer. Characteristic wavelength 589 nm.

Morphology of the supports and mapping of the elemental composition was done by SEM-EDAX analysis at SICART, Vallabh Vidyanagar, Gujarat, India. A FEG Nano Nova 450 with EDAX; accelerating voltage 20V to 30 kV, beam current 200μA; 25-1000000x magnification; resolution 1.0 nm at 15kV to 3.5 nm at 100V instrument was used for measurement.

Carbon, hydrogen and nitrogen of the supports were determined with a Perkin Elmer Model 2400 Series II absolute CHN analyzer at SICART Vallabh Vidyanagar, Gujarat, India. Temperature of the sample was ramped to 2000°C.

A Perkin Elmer Spectrum GX instrument FTIR was used for Fourier Transform IR spectroscopy measurements. The samples were analyzed as wafers prepared with KBr as a medium. This facility is available at SICART Vallabh Vidyanagar, Gujarat, India.

While NH_3 TPD is widely used for determining acidity of solid oxide materials, model test reactions provide additional information. The chemical acid-base nature of these materials was studied through a model reaction, decomposition of MBOH (2-methyl-3-butyn-2ol). This reaction was first reported by H. Pernot et.al. from Rhone-Poulenc [31]. MBOH is reported to convert to MByne [3-methyl-3-buten-1yne] over acid sites, to HMB [3-hydroxy-3-methyl-butanone] and MiPK [3-methyl-3-buten-2-one] over amphoteric sites and to acetylene and acetone over basic sites. This model reaction is convenient in investigating the acid-base nature of solids.

Conversion and product selectivity were calculated using the equations given below.

$$conversion\ of\ MBOH = \frac{concentration\ of\ MBOH\ in\ reactant - concentration\ of\ MBOH\ in\ product}{concentration\ of\ MBOH\ in\ reactant} \times 100 \quad \textit{Equation 1}$$

$$Product\ selectivity\ Si = Mol\ component\ 'i'\ produced \div mol\ \text{MBOH}\ converted \quad \textit{Equation 2}$$

The rate of deactivation of the supports for decomposition of MBOH was determined by fitting the activity data to an empirical Power law equation.

$$A = c \times t^{kd} \quad \textit{Equation 3}$$

Wherein A is the activity at time t. It is determined as the ratio of conversion at any time t / initial conversion, t = time on stream (min), kd is the decay constant and c is a scaling factor which is constant.

2.4 Results and Discussion

2.4.1 Chemical composition of supports (by ICP and flame photometer)

Composition of the supports in weight percent on dry basis (as oxide) is given in Table 2.2 below.

	ZrO_2 (%)	Al_2O_3(%)	Na_2O(%)
GA-7	52.1	46	2.05
GA-8	53.2	45.1	2.2
GA-9	52.3	44	3.9
GA-10	53	45.1	2.7
ZrO_2-7	96.3	0.0	3.7
ZrO_2-8	96.7	0.0	3.3
ZrO_2-9	95.6	0.1	4.3
ZrO_2-10	94.5	0.1	5.4
AT-7	53.4	42.8	3.8
AT-8	52.0	42.7	5.3
AT-9	52.3	43.1	4.6
AT-10	48.2	47.0	4.8
AM-7	50.2	46.8	3.0
AM-8	49.1	47.7	3.2
AM-9	47.4	48.7	3.9
AM-10	48.2	47.5	4.3
CP-7	51.7	43.6	4.7
CP-8	47.6	48.5	3.9
CP-9	51.9	43.0	5.1
CP-10	50.0	44.3	5.7
GA-PHY-7	53.2	44.1	2.7
GA-PHY-8	52.1	44.6	3.3
GA-PHY-9	50.9	43.2	5.9
GA-PHY-10	51.9	41.3	6.8

Table 2. 2: Composition of zirconia-alumina bi-component supports

Volatiles were removed by calcining the samples at 750°C for 8h. The samples were digested in aqua regia and further diluted with Millipore water. Zirconium and aluminum were analyzed through ICP-OES while sodium was measured by Flame Photometry. Results showed that all the samples irrespective of whether they were prepared by deposition-precipitation or co-precipitation, had a composition ZrO_2 50±3%; Al_2O_3 43±3% and Na_2O 5±3% (on weight basis). The values of the former two are close to those based on the input raw materials used for preparation. Based on input the theoretical composition is expected to be 54.7 wt% ZrO_2 and 45.3 wt% Al_2O_3. The zirconia content of the samples of neat zirconia (ZrO_2 series) varied from 94-97 wt. %. Na_2O accounted for the balance. It increased as the pH of preparation was increased.

The presence of sodium (expressed as Na_2O) proportionately decreased the concentrations of the zirconium and aluminum oxides. It was observed that the pH of precipitation and the substrate used had a combined effect on the soda content of the bicomponent support samples. Sodium appeared to be strongly occluded because it was present even after washing the precipitate thrice with hot demineralized water (80°C). Zirconium carbonates are reported to form non-stoichiometric solids which contain alkali ions[32]. Preparation of sodium zirconium carbonates is reported in European patent specification 0004403 B1[33]. The inventors of this patent Mc. Arthur et al. have cited work of Pospelova and Zaitsev[34] wherein this compound is described by an empirical formula $Na_4[ZrOZr(OH)_2(CO_3)_4].8H_2O$. In US patent 6627164B1[35] R. Wong has described the preparation of sodium zirconium carbonate which is free of hydroxyl groups. It is described as an amorphous polymeric compound with formula $NaZrO_2CO_3.nH_2O$. Its preparation involves heating a mixture of zirconium oxychloride and sodium carbonate at temperature 65-121°C and acidic pH 3.5 to 7, preferably 6.0. In the present study, precipitation was carried out in pH range 7-10 hence it is expected that sodium zirconium carbonate formed would be similar to $Na_4[ZrOZr(OH)_2(CO_3)_4].8H_2O$. This is supported by results of evolved gas analysis by TGA-MS (details in later section of this chapter) in the present study, which shows the evolution of water and CO_2 which indicates the presence of hydroxides and carbonates in all the samples irrespective of the pH of precipitation. Presence of nitrates was also detected from the evolution of NO in all the samples. The source of nitrates is believed to be $NaNO_3$ which is occluded in the support. It is a by-product of precipitation.

The residual Na_2O content in the supports is dependent on method of precipitation, the alumina substrate used and the pH of precipitation. Samples prepared by deposition-precipitation

(DP) using GA substrate showed least residual Na_2O amongst all samples when it was prepared at pH>8, while bi-component supports prepared by physical mixing (PHY) and co-precipitation(CP) showed highest residual Na_2O. This indicates better dispersion of zirconia on GA substrate when DP method is used, which facilitates ease of the washing of Na_2O from the precipitates. Also the higher residual Na_2O in physical mixing method and neat ZrO_2 samples suggest that precipitates of ZrO_2 are gelatinous in nature rendering washing less effective. This also results in low surface area of these samples after drying and calcination.

2.4.2 Nitrogen Physisorption (BET SA, N_2 Pore volume and pore size):

The bulk density of the alumina substrates was 0.9 g/ml for ATH, 0.4 g/ml for AM and 0.5 g/ml for GA. Surface area and pore volume of the substrates were 20, 300 and 250 m^2/g and 0.015, 1.02 and 0.85 ml/g respectively.

The trend of specific surface area as a function of pH for the five series of supports is shown in Figure 2.3. Values for the neat substrates are also provided in this plot. General trends are:

Specific surface area of AM (S) > GA(S)>>> AM series ≥ GA-PHY series ≥GA series >> CP series>>> AT series~ AT (S) ≥ ZrO_2 series

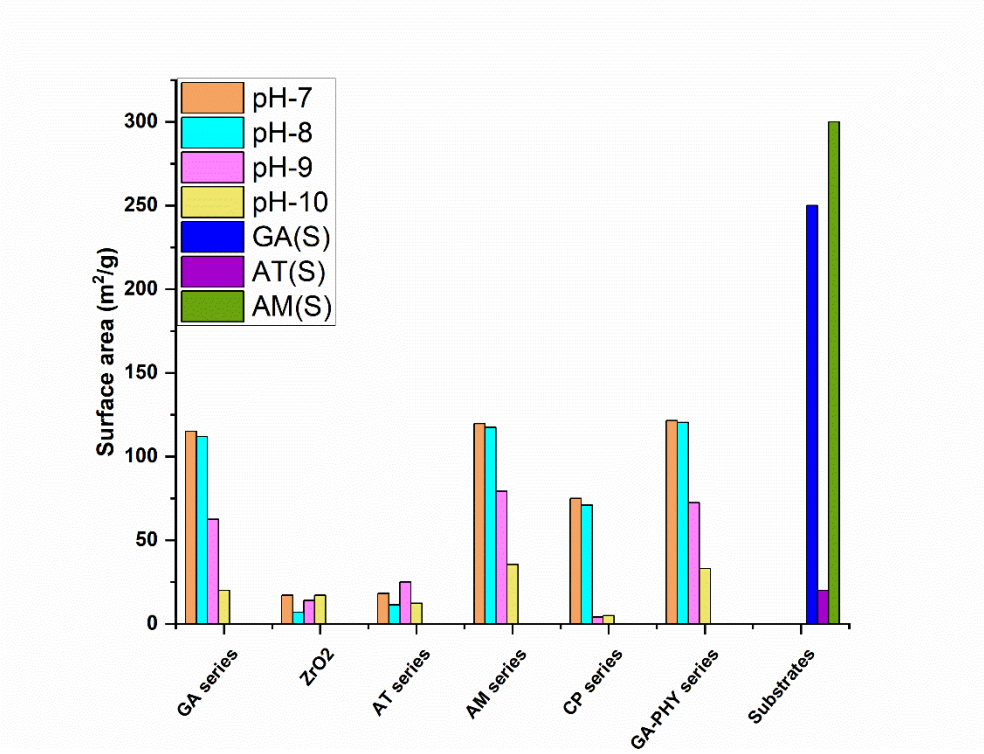

Figure 2. 3: Specific surface area of support samples

Samples of neat zirconia prepared across the pH range studied (ZrO_2-7 and ZrO_2-10) in the present study have low surface area 17 m^2/g (both). Z. Feng et al. have prepared precipitated zirconia from 5 wt% aqueous zirconyl nitrate using 1.5 wt% aqueous ammonium hydroxide with final pH adjusted to pH 8 using nitric acid and also sol-gel zirconia by base hydrolysis of zirconium isopropoxide. They have reported BET specific surface area 35 and 24 m^2/g for samples which were calcination at 500°C for 3h[36]. The specific surface area of samples of precipitated zirconia prepared in the present study is in the ballpark range of these values. The supports of the present study were calcined at 350°C for 8 hours.

From results presented in Figure 2.3, for a given series of the bi-component zirconia-alumina supports which are prepared using the same substrate, the specific surface area is higher when the final pH of precipitation is ≤8 and it decreases sharply when final pH (of preparation) is above a value of 8 indicating difference in the physico-chemical nature of the precipitate.

The substrates AM(S) and GA(S) have moderate to high surface area 250-300 m^2/g. The bi-component zirconia-alumina supports which are prepared using these two substrates present specific surface areas in the range 20 to 121 m^2/g depending on the final pH of preparation. This corresponds to a specific surface area of about 40-50% relative to substrate for bicomponent supports prepared by deposition-precipitation at pH 7-8, about 25-28% for supports prepared at pH 9 and 8-13% for supports prepared at pH 10. These values largely lie between those of these substrates and neat unsupported zirconia i.e. ZrO_2 series

Series AT is an exception. The specific surface area of the substrate AT(S) itself is low ~20 m^2/g. The specific surface area of the AT series of supports is comparable to that of the substrate and there is no appreciable trend with pH of precipitation. Surface area of substrate AT(S) imparts very marginal to no advantage of specific surface area to the bi-component system, that too when pH of precipitation is <8. The specific surface area of neat zirconia ZrO_2-7 is 17 m^2/g when it is precipitated at this pH while that of the bi-component supports AT series is around 11-25 m^2/g.

Thus, deposition-precipitation of zirconia on to AM(S) and GA(S) helps to realize overall surface areas which are significantly higher than those of neat ZrO_2 series which are prepared by precipitation. This advantage diminishes when pH of preparation exceeds 8, and is substantially

diminished in supports which are precipitated at pH 10. The precipitate of samples prepared at pH >8 was observed to have gel-like texture. Materials with this texture are known for their behavior to shrink significantly during drying. The shrinkage results in loss of specific surface area of the dried product.

Samples prepared by physical mixing i.e. GA-PHY series are having surface area slightly higher to GA series samples mostly because of the lower interaction of zirconia and alumina.

Supports prepared by co-precipitation (CP series) at pH 7 or 8 have specific surface area ~70-75 m^2/g. This is about half that of the corresponding GA, GA-PHY and AM series (which are prepared by deposition-precipitation) but significantly higher than that of AT series or the neat ZrO_2 samples. Surface area of the CP series decreases drastically to 4-5 m^2/g when the pH of preparation exceeds 8. The specific surface area of these samples is significantly smaller than that of supports prepared by deposition-precipitation and even neat monocomponent ZrO_2 supports (at pH 9-10). Thus the trend of specific surface area of the supports with the method of their preparation decreases in the order Deposition-precipitation > Co-precipitation > strike precipitation (neat zirconia).

Trends of specific pore volume as a function of pH of precipitation are given in Figure 2.4 below. The pore volumes of all alumina substrates and neat zirconia (ZrO_2) are 0.015 ml/g AT(S), 1.02 ml/g AM(S), 0.85 ml/g GA(S) and ~0.013-0.017 ml/g ZrO_2 series. Pore volumes of the bicomponent series of supports are observed to be significantly lower than that of the neat substrates AM(S) and GA(S). The GA-PHY and GA series of bi-component supports present a decrease in the range of 63-91% in pore volume relative to substrate with increasing pH whereas the AM series presents a decrease in the range of 85-94% relative to the substrate as pH of preparation is increased from 7 to 10. The AT series however show a slight increase in pore volume relative to the substrate.

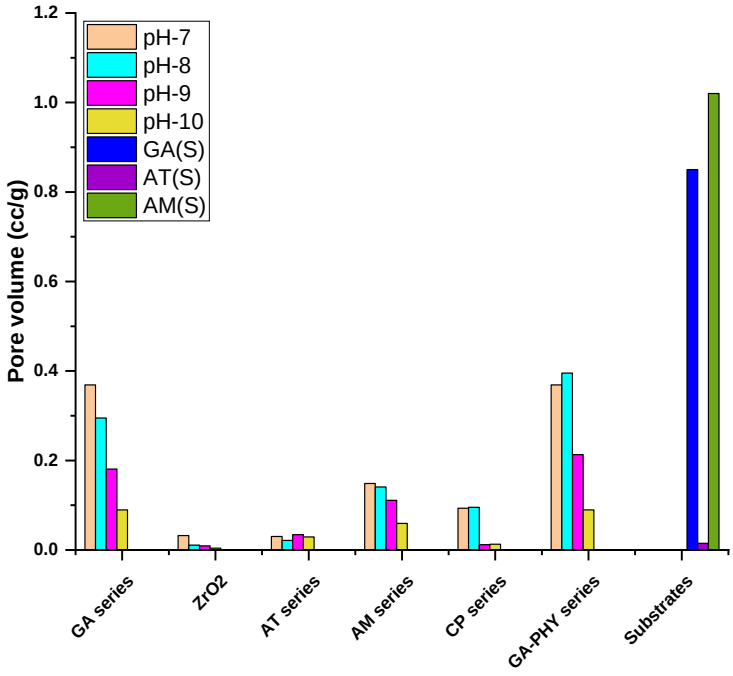

Figure 2. 4: Trend of pore volume with pH of precipitation

The GA-PHY and GA series are prepared with the same substrate, viz. gamma-alumina, with the difference that the GA-PHY series was prepared by physical mixing of freshly precipitated zirconia with slurry of gamma-alumina whereas the GA series was prepared by deposition-precipitation of zirconia from a slurry onto gamma alumina. The former series shows 10% higher pore volume than the latter series for samples which are prepared at final pH ≤8. This difference is not observed when the final pH of precipitation is >8. Further, a sharp decrease in pore volume is observed for all the series of supports when the final pH of precipitation exceeds 8, which is attributed to gelatinous nature of the gel of zirconia when the final pH of precipitation is >8. These observations indicate that the decrease could be due to blockage of pores of the substrate by the precipitate of zirconia for supports which are prepared at the higher values of pH.

Pore volume of the AM series (Figure 2.4) also shows a sharp decrease relative to substrate AM(S). AM(S) substrate is a pseudoboehmite (oxyhydroxide of aluminum). It readily peptizes in acidic and alkaline solutions. Peptization is local dissolution of the oxyhydroxide to form ‘sol-like’ species of aluminum. This is aggravated at elevated temperature. Peptization is an important

property in preparing formed bodies of alumina (such as extrudates) for use as catalyst supports in fixed bed catalytic applications. Thus, the large decrease in pore volume (Figure 2.4) and pore diameter (Figure 2.5) of bicomponent AM series is attributed to destruction of the microstructure of AM(S) substrate at the initially acidic and finally alkaline conditions of precipitation at elevated temperature (60°C).

The pore volumes of CP series decrease from about 0.1 ml/g at pH of preparation 7-8 to 0.012-0.013 ml/g at pH 9-10. The CP-series shows pore volumes which are significantly lower than those prepared by deposition-precipitation on AM(S) and GA(S) substrates. The decrease in pore volume with increase in pH from 8 to 9 is also substantially higher for this series.

Average pore diameter was calculated using the Gurvich relation D = 4V/Specific surface area. Trends of the average pore diameter versus pH of precipitation for the three different substrates is shown in Figure 2.5 below. Values of average pore diameter of the substrates AT(S), AM(S) and GA(S) are also included in the plot as point data.

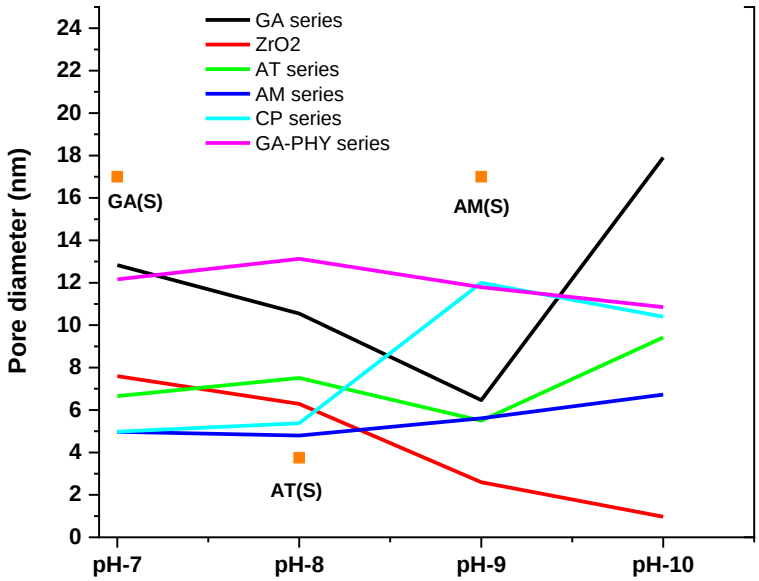

Figure 2. 5: Average pore diameter of bicomponent zirconia-alumina supports.

As seen from Figure 2.5 above, the average pore diameter of the monocomponent ZrO_2 series decreases sharply with increasing pH. This is attributed to increasing gel-nature of the precipitate with increasing pH which results in shrinkage during drying. The bicomponent zirconia-alumina supports mostly show an overall increase (or no significant decrease relative to neat ZrO_2) with increasing pH. Thus, deposition-precipitation is advantageous in achieving a larger pore diameter.

Amongst the bicomponent series, the average pore diameter of the AM series increases with pH, however this series shows the smallest average pore diameters. Comparing this with the pore diameter of the substrate AM(S), it is observed that there is a drastic decrease in pore diameter when zirconia is introduced by deposition-precipitation. Pore volume of the AM series (Figure 2.4) also shows a similar sharp decrease relative to substrate AM(S). As explained in the section of pore volume, this behavior is attributed to the ease of peptization of AM(S). Thus, the large decrease in pore volume and pore diameter of bicomponent AM series is attributed to destruction of the microstructure of AM(S) substrate at the initially acidic and finally alkaline conditions of precipitation at elevated temperature (60°C).

The GA and GA(PHY) series on the other hand show a much smaller decrease of pore volume and average pore diameter relative to the substrate than the AM series. GA-9 shows deviation, which could be due to pore plugging. The GA substrate is a transition alumina (γ-form) which is not expected to peptize as readily as pseudoboehmite, which explains retention or small decrease in average pore diameter and pore volume (relative to the value of the substrate) after incorporating zirconia.

The AT series shows an increase in pore diameter with increasing pH of precipitation. AT(S) is a trihydroxide of aluminum and it is not expected to peptize. Since the average pore diameter of the AT series is larger than the AT(S) substrate, the increase is attributed to contribution from zirconia.

The CP series shows smaller average pore diameters than that of the GA or GA(PHY) series at pH 7-8, whereas pore diameters are comparable with GA(PHY) at pH 9-10. The substantial increase in pore diameter correlates with the attendant sharp drop in specific surface area (Figure 2.3).

In deposition-precipitation zirconia is expected to deposit over the alumina substrate. Considering the low surface area and pore volume of neat precipitated zirconia (ZrO_2 series), the

increase of these parameters in the bicomponent series of supports prepared by deposition-precipitation shows that this method is advantageous.

2.4.3 SEM-EDAX

In order to check for homogeneity at local level EDAX studies were carried out for support series GA and GA(PHY). EDAX profiles are presented in Figure 2.6 and Figure 2.7 while data is compiled in Table 2.3.

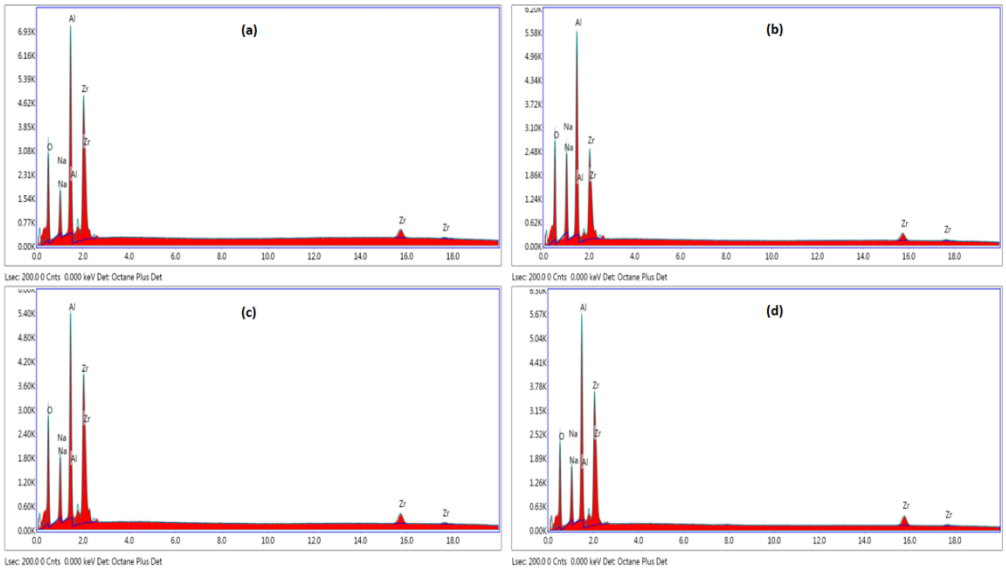

Figure 2. 6: EDAX analysis of (a) GA-7 (b) GA-8 (c) GA-9 (d) GA-10

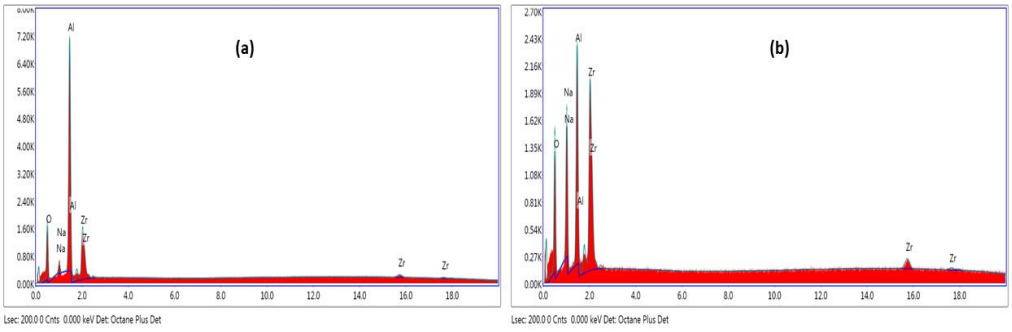

Figure 2. 7: EDAX analysis of (a) GA(PHY)-7 (b) GA(PHY)-10

An area of 285 µm x 207 µm was mapped for each of the samples. Results of EDAX are summarized in Table 2.3 below. EDAX confirms the presence of sodium, zirconium, aluminum

and oxygen in all six samples. The sodium appears to be present in occluded form which is difficult to wash out with hot water. Atom ratios of Na/Zr and Zr/Al calculated from results of EDAX are presented in Table 2.3.

Support	Na/Zr (Atomic)	Zr/Al (Atomic)
GA-7	0.97	0.69
GA-8	2.04	0.56
GA-9	1.2	0.79
GA-10	1.1	0.77
GA-PHY-7	1.29	0.21
GA-PHY-10	2.39	0.71

Table 2. 3: Calculated Na/Zr and Zr/Al atomic ratio of zirconia-alumina bi-component supports from EDAX data

As seen from Table 2.3 above, the atomic ratio of Na/Zr varies from 0.97 to 2.04 in case of the GA-series and from 0.97 to 2.39 in the case of GA(PHY) series. It was observed from the combined results of CHN and ICP-OES (refer Table 2.5 below) that the sodium appears to exist as its nitrate, so, there is no association between Na and Zr contents.

Based on the bulk compositions of the bi-component series of supports determined by ICP-OES (Table 2.2), the Zr/Al atomic ratio of these samples varies from 0.47 to 0.49 with average value 0.486 and standard deviation 0.01. The Zr/Al atomic ratio measured from EDAX (Table 2.3) ranges from 0.56 to 0.79 with an average of 0.70 and a standard deviation of 0.104 for the GA series. In the case of the GA-PHY series the Zr/Al atom ratio shows a significantly higher variation than the GA series. It varies from 0.21 to 0.71 with an average of 0.35 and a standard deviation of 0.245. The high variation in Zr/Al atom ratio in the results of EDAX for GA-PHY series indicates heterogeneity of composition at a local level. This is attributed to the GA-PHY series being prepared by physically mixing powder of γ-Al_2O_3 with precipitate of zirconium. Thus, based on the results of EDAX, it is clear that the GA series of supports which are prepared by deposition-precipitation have better homogeneity at a local/microscopic level than the GA-PHY series.

2.4.4 Thermogravimetry

2.4.4.1 DTG-DSC

Figures 2.9, 2.10 and 2.11 show the derivative of weight loss (%/°C) and associated heat flow (W/g) i.e. DTG and DSC pattern comparison for series GA and ZrO_2 series, AT, AM and GA series, GA, GA-PHY and CP series respectively. The corresponding figures of the substrates AT(S), AM(S) and GA(S) are shown in Figure 2.8. The temperature of peak weight loss provides an indication of relative strength of adsorption of species which desorb or energy required for decomposition. Weight change provides information about quantity of a particular chemical species.

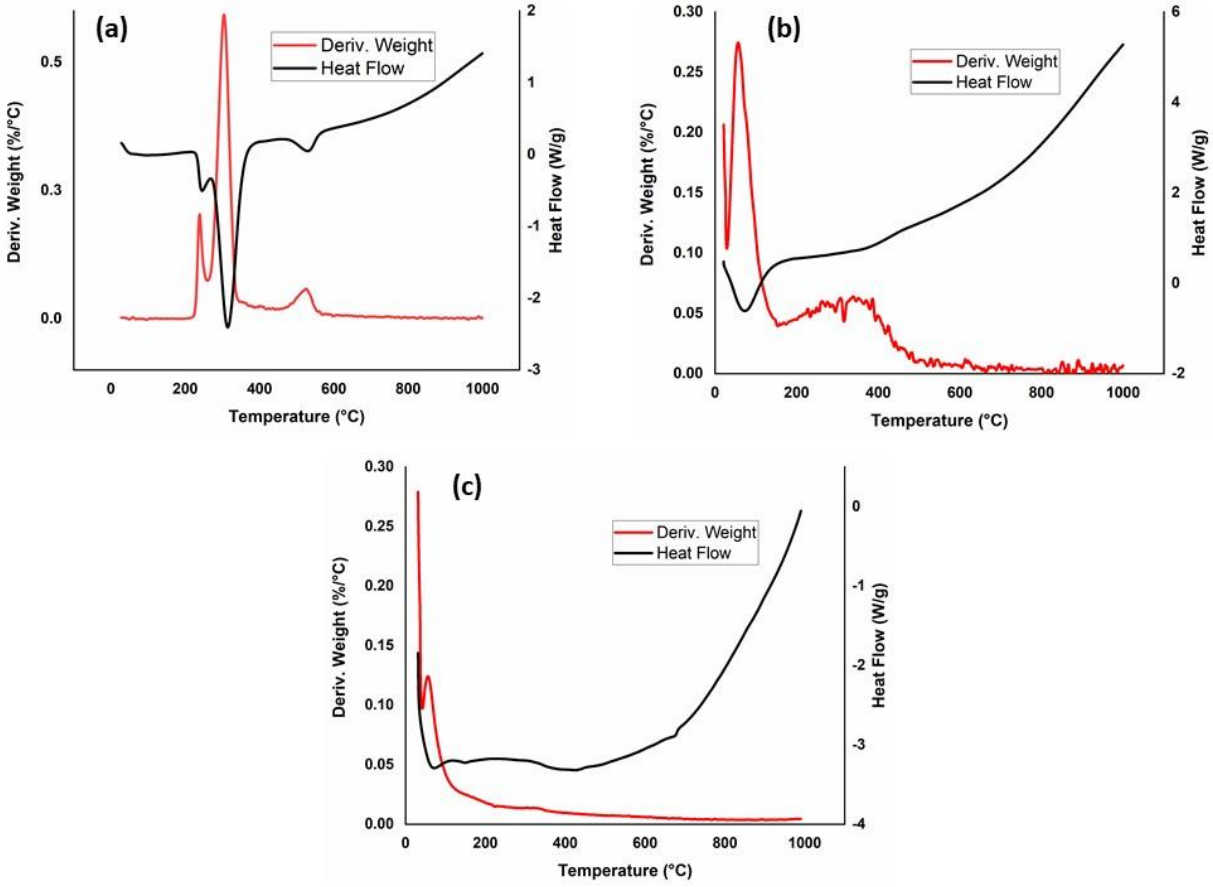

Figure 2. 8: DTG-DSC of alumina substrates used for deposition-precipitation (a) AT(S) (b) AM(S) (c) GA(S)

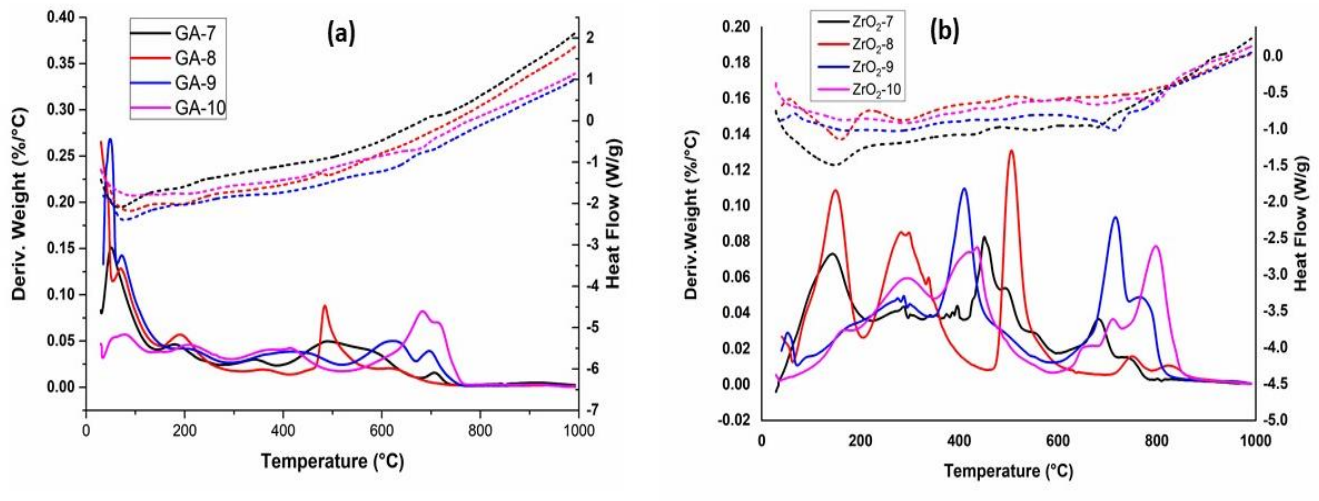

Figure 2. 9: DTG-DSC comparison of (a) GA series and (b) ZrO_2 series samples

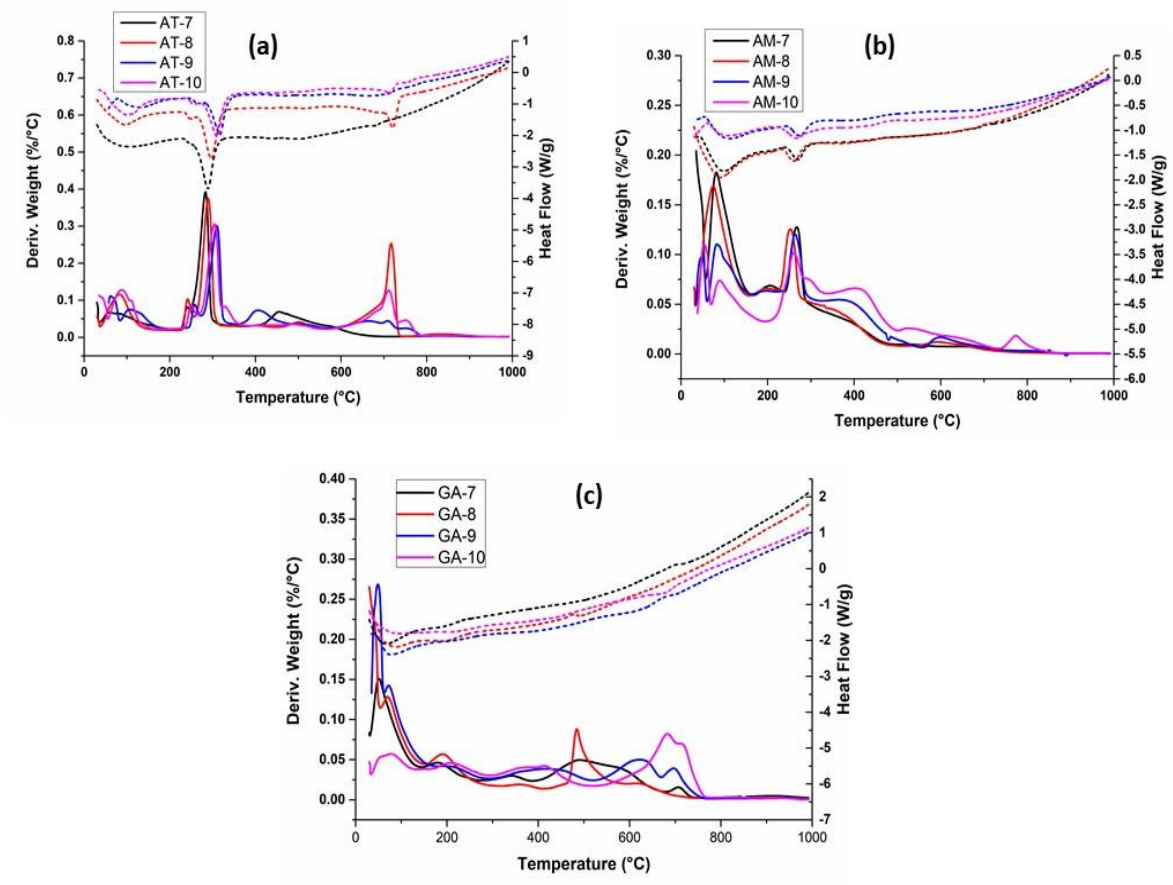

Figure 2. 10: DTG-DSC of supports prepared by deposition-precipitation using different alumina substrates (a) AT series (b) AM series (c) GA series

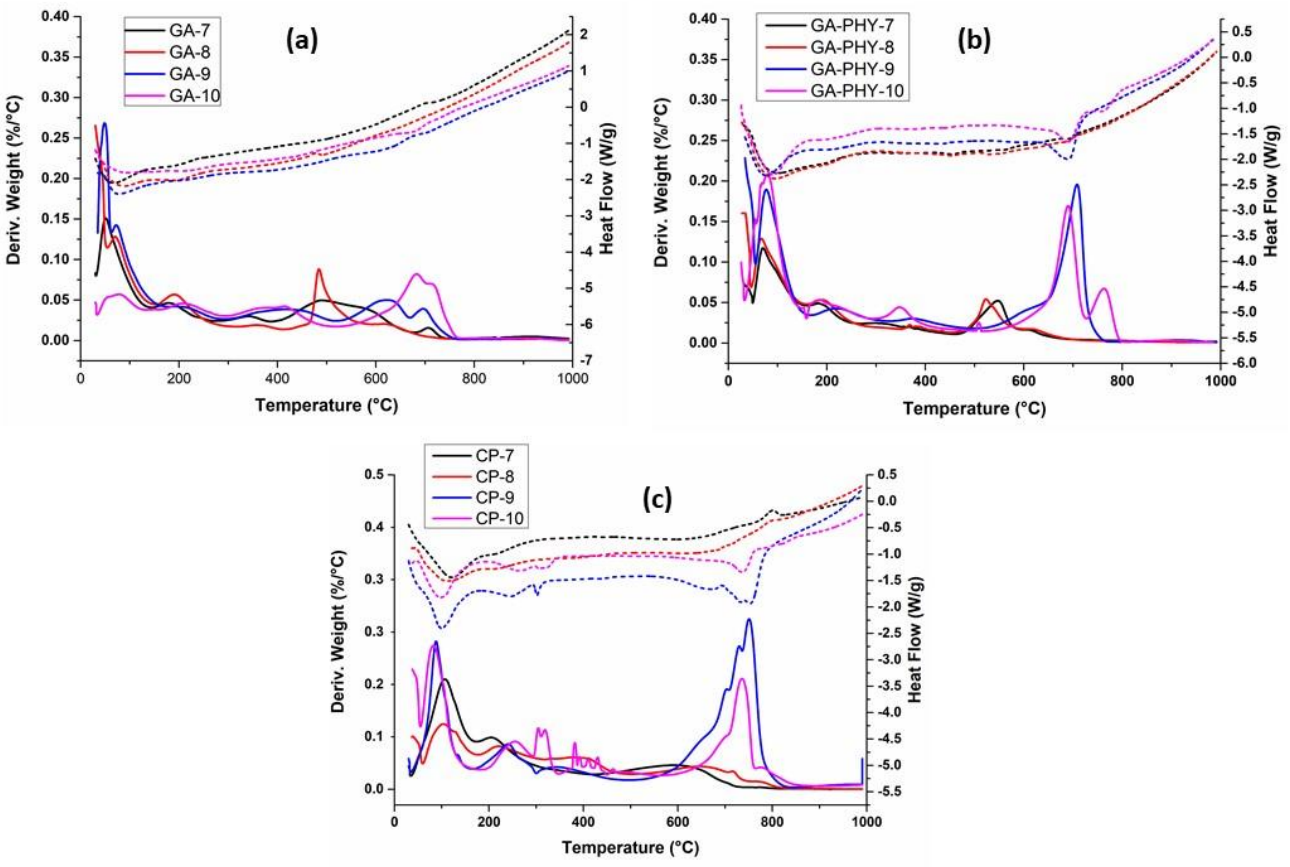

Figure 2. 11: DTG-DSC of supports prepared by different methods (a) GA series – Deposition-Precipitation method (b) GA-PHY series – Physical Mixing method (c) CP series – co-precipitation method

1. Peaks with Tmax <200°C : these peaks are attributed to loss of physisorbed water/dehydroxylation (based on results of TGA-MS; Figures 2.14 and 2.15)

As seen from Figures 2.8 a, b, c: for peaks at <200°C the derivative of weight change of substrates show the trend GA(S) (99°C) > AM(S) (61°C). AT(S) does not show any peak in this temperature range. The lower temperature of AM(S) is consistent with it being a oxyhydroxide, whereas GA(S) is a dehydroxylated form of AM(S) viz. γ-Al_2O_3. This peak is attributed to loss of physisorbed water in both the GA(S) and AM(S) and partial dehydroxylation in case of AM(S). AT(S) does not appear to have any physisorbed water and also does not dehydroxylate at these temperatures.

As observed from Figures 2.9, 2.10 and 2.11, for peaks at <200°C, the trend of Tmax of desorption/dehydroxylation is ZrO_2 series(150-160°C) > CP series (90-110°C ≥ AT series (70-110°C) > GA-PHY series (80-95°C) ≥ AM series (60-93°C) ~ GA series (60-90°C). Thus, neat ZrO_2 requires significantly higher energy for dehydroxylation compared to the bicomponent supports. Thus, there is a distinct difference in chemical moiety of zirconia between the monocomponent and bicomponent supports. Further, from Figure 2.9 b it is observed that the ZrO_2 samples precipitated at pH 7-8 show significantly larger peaks than those precipitated at pH 9-10. This correlates with the presence of higher fraction of zirconium hydroxide in these supports which are prepared at lower pH. The distribution of zirconium hydroxide and zirconium carbonate (as determined by CHN and ICP-OES) is given in Table 2.5. No significant difference in Tmax is observed across the three bicomponent support series which are prepared by deposition-precipitation using different substrates (Figure 2.10 a, b, c). The peak at about 60°C for AM(S) reflects in the AM series. The CP series, which is prepared by co-precipitation (Figure 2.11c) shows peaks in almost the same temperature range as samples prepared by deposition-precipitation (Figure 2.10a, b, c). In summary, there is a clear difference in the TGA behavior between neat zirconia and bicomponent zirconia-alumina supports.

2. **Peaks with Tmax between 200-400°C:** These peaks are attributed to dehydroxylation of the supports (based on results of TGA-MS; Figures 2.14 and 2.15)

From Figure 2.8 a, b, c it is observed that for peaks in the range 200-400°C the GA(S) substrate does not show any peak whereas AT(S) shows sharp endothermic dehydroxylation in two stages, 242°C (minor) 301°C (major). This is attributed to dehydroxylation of the trihydroxide. AM(S) shows a weak broad peak from 200°C-400°C with maxima at about 360°C which is also attributed to dehydroxylation as it transitions to γ-Al_2O_3.

The bi-component zirconia-alumina samples (refer Figures 2.9 a, b, Figure 2.10 a, b, c and Figure 2.11 a, b, c) show the trend GA series(185°C-210°C; 330-420°C) weak = GA-PHY series (195°C-220°C, 350°C-370°C) weak > AT series (280°C-310°C) strong >ZrO_2 series (280°C-300°C, 410°C-420°C) strong >AM series (250°C-280°C) strong >CP series (205°C-255°C mod, 350-400°C weak). Most of the samples show peaks in two distinct temperature regions, one closer to 200°C and the other closer to 400°C. A good match between Tmax of AT(S) substrate (Figure 2.8a) and AT series (Figure 2.10a) indicates contribution of dehydroxylation of AT(S) substrate in

the AT series of supports. Since the GA(S) substrate (Figure 2.8c) does not show any signal in this region, the peaks in the GA and GA-PHY series (Figure 2.11a, b respectively) are attributed solely to dehydroxylation of zirconia. In the case of AM series (Figure 2.10b) there is contribution from both zirconia and AM substrate (dehydroxylation to γ-Al_2O_3). Based on results of TGA-MS, of the two peaks, the peak at lower temperature is attributed to dehydroxylation and the one at higher temperature to decarboxylation and/or dehydroxylation. Interestingly, the peak position of ZrO_2 series (Figure 2.9b) differs significantly from that of all the bicomponent zirconia-alumina supports prepared by deposition-precipitation (Figures 2.10 b, c and Figure 2.11 a, b, c) except AT series, therein indicating some interaction between zirconia and the GA(S) and AM(S) alumina substrates. XRD data supports this observation. In case of AT series (Figure 2.10a) the peaks from 280-310°C are due to dehydroxylation of aluminum trihydrate. The CP series (Figure 2.11c) which is prepared by co-precipitation show peaks whose positions and intensities are distinctly different from that of the other series, indicating formation of different species, probably solid solution of Al and Zr. XRD data shows its formation. The AT, GA, AM and CP series (Figures 2.10 and 2.11) show a shift of peak maxima to higher temperature when pH increases from 7-8 to 9-10 indicating increase in strength of interaction with support. GA-PHY series (Figure 2.11b) does not show peaks at pH 7-8, reason for which is not clear. ZrO_2 series (Figure 2.9b) does not show any change in peak Tmax with pH in this temperature region. Thus, it appears that there is some interaction between ZrO_2 and Al_2O_3. GA, GA-PHY, AM and CP series (Figures 2.10 and 11) of supports show peaks at lower temperature than ZrO_2 (Figure 2.9b) indicating weaker hydroxyl bonds than ZrO_2 series.

3. **Peaks with Tmax between 400-600°C**: These peaks are attributed to decarboxylation and/or dehydroxylation (based on results of TGA-MS; Figures 2.14 and 2.15)

As seen from Figures 2.8 a, b, c the substrates do not show any peaks in this region. As seen from Figures 2.10 and 2.11 the bicomponent supports prepared by coprecipitation (CP series) or deposition-precipitation (AT, AM, GA, GA(PHY) also show very weak broad peaks in this region. Monocomponent ZrO_2 series (Figure 2.9b) shows strong peaks in this temperature region across the entire range of pH studied. This indicates that these species (which are carbonates based on results of TGA-MS) are much lower in concentration or absent when the supports are prepared by

deposition–precipitation or coprecipitation. This indicates chemical interaction between Al and Zr which retards formation of these carbonate species of zirconia. Peaks for samples prepared at pH 7-8 (supports ZrO_2-7 and ZrO_2-8, Figure 2.9b) are at higher temperature (470 °C-510°C) while samples precipitated at pH 9-10 (ZrO_2-9 and ZrO_2-10) are at 405°C-430°C indicating stronger bonds in case of the former. AM series show broad diffuse peaks in this region. Intensity of peaks of samples prepared at pH 9-10 is higher. AT series (Figure 2.10a) show weak peaks in the 400°-500°C range. Samples prepared at pH 7-8 show peaks at higher temperature, GA-PHY series (Figure 2.11b) shows peaks in the 500°C-600°C range for samples prepared at pH 7-8, whereas those prepared at pH 9-10 do not show any peaks, GA series (Figure 2.11a) precipitated at pH 7-8 show peaks at about 490°C-495°C whereas those precipitated at pH 9-10 show broad diffuse peaks (420°C-430°C) in this region. The weak nature of peaks as well as broadening makes it difficult to draw trends. In general supports prepared at lower pH (7-8) show peaks at higher temperature. At best, temperature trend is GA-PHY (520°C-550°C) >ZrO_2 (410°C-510°C)>AT (405°C-460°C) > GA (440°C) > AM (380-410°C).

4. **Peaks with Tmax between 600-800°C:** These peaks are attributed to decarboxylation and denitrification (based on results of TGA-MS; Figures 2.14 and 2.15)

As seen from Figures 2.8 a, b, c the substrates do not show any peaks in this region. ZrO_2 (Figure 2.9b), CP (Figure 2.11c), AT (Figure 2.10a) and GA(PHY) series (Figure 2.11b) show relatively intense peaks in this temperature region. In comparison, the remaining supports prepared by deposition-precipitation (AM, GA which are high surface area substrates, Figures 2.10 b, c) show peaks of low intensity. Peak intensities increase with pH of precipitation for all the series (Figures 2.9, 2.10, 2.11). Peak positions also shift to higher temperature with increasing pH in most of the cases. Exact reason for this is difficult to identify because both (hydroxy)carbonates and nitrates decompose in this region. Based on discussion in CHN section (Table 2.5), there is a shift from hydroxide to carbonate species of zirconium with increasing pH. Further, $NaNO_3$ appears to occlude. Multiple peaks are observed in the ranges 595°C-620°C (AM series), 650°C-700°C (AM, GA, CP, ZrO_2, GA(PHY) series, 705°C-720°C (all except AM and GA-PHY), 750°C-770°C (AT, AM, CP, ZrO_2, GA-PHY) and 820°C (ZrO_2). These peaks could not be individually assigned to either the decomposition of carbonates or nitrates. However, it is broadly evident from TGA-MS (Figures 2.14 c, d and 2.15 c, d) that peaks at about 580°C, 600°C and 680-720°C are

due to denitrification and those in the region 330°C, 380°C, 500°C, 690-760°C are due to decarboxylation.

Endothermic peaks are observed in all the samples which correspond with weight loss. These are understandably due to thermal dehydroxylation, decarboxylation and denitrification (as seen from results of TGA-MS, Figures 2.14 and 2.15). Only samples CP-7 and CP-8 (Figure 2.11c) showed clear exotherms at about 820°C, which indicate phase transition. Since these are absent in the substrates (Figure 2.8 a, b, c), they may be assigned to phase transition of ZrO_2. The remaining CP series (Figure 2.11c), and all samples of ZrO_2 (Figure 2.9 b), GA-PHY (Figure 2.11 b) and GA series (Figure 2.11a) show a drift of baseline in the exothermic direction at >700°C, which could be due to slow phase transformation. This trend is less prominent in the AT (Figure 2.10a) and AM series (Figure 2.10b). The AM series (Figure 2.10b) showed weak exotherms at about 500°C which can be attributed to phase transition to gamma alumina. AT(S) (Figure 2.8 a) shows an endotherm with slight weight loss which can be attributed to phase transition to CHI-Al_2O_3 at about 540°C. AM(S) (Figure 2.8b) shows slight hint of an exotherm at about 480°C which can be attributed to phase transition to γ-Al_2O_3 [37].The temperatures of transition are consistent with literature reports[37]. A continuous drift in the heat flow plot (W/g) is observed at higher temperatures which can be attributed to slow transition to α-Al_2O_3 which is the most stable thermodynamic phase of Al_2O_3. The γ-Al_2O_3 sample too shows this behavior as is expected.

The DSC shows low intensity peaks which are exothermic by nature. These are observed at about 250°C, 470°C and 680°C in the ZrO_2 series (Figure 2.9 b). These are attributed to phase transition from amorphous to tetragonal ZrO_2. Similar transitions are reported by Stenina[27] and Zhou[38] in the same temperature range. Results of XRD confirm the presence of tetragonal phase of zirconia in samples which are calcined at 550°C (Figures 2.22 a, b, c) in the current study.

The trend of total weight loss of alumina substrates used for deposition-precipitation is AM(S) (36.4%) >AT(S) (34.5%) > GA(S) (14.8%) (Refer Figure 2.12 below). This is in line with expectation based on their hydroxyl content and physisorbed moisture. The major weight change occurs at <200°C for GA(S) and AM(S) (refer Figure 2.8b and c). It is due to loss of physisorbed moisture in case of the former and due to dehydroxylation of the oxy-hydroxide in case of the latter. AT(S) does not show any weight loss in this temperature range. It occurs between 200-400°C for AT(S) (Figure 2.8b). This is attributed to dehydroxylation. Transition aluminas viz. CHI

in case of AT(S) and γ-Al_2O_3 in case of AM(S) form prior to complete transformation to α-Al_2O_3 if heated to temperature above 900°C.

TGA of the samples prepared by deposition-precipitation and co-precipitation are shown in appendix 1. The gist of weight loss in different temperature regions from these figures is captured in the form of bar charts below. As seen from Figure 2.12, the trend of total weight loss of the bi-component supports between series is ZrO_2 (25.9-28.8%) < GA (25.5-31.6%) < AM (30.6-31.9%) < GA-PHY (21.8-40.5%) < AT (34.1-40.6%) <CP (33.4-51%).

Chuanyong Huang et. al. have studied hydrous zirconia ($ZrO_2.xH_2O$) and zirconium hydroxide ($Zr(OH)_4.xH_2O$)[39]. The former was prepared by reverse strike precipitation, adding zirconium oxychloride to a solution of NaOH[40] whereas the latter was prepared by a forward strike precipitation addition of NH_4OH to a solution of $ZrOCl_2.8H_2O$ till final pH 9. The TGA studies reported by them show that both materials dehydroxylate almost completely at 400 °C. The total weight loss of the former is reported as 21.5% whereas the weight loss of the latter is reported as 32.2%. The total weight loss of ZrO_2 series supports prepared by precipitation in the current study (Figure 2.12) is 25-28 wt% which is closer to that of $Zr(OH)_4.xH_2O$. Incidentally the samples of the current study were also prepared by forward strike precipitation. However, it is noted that TGA-MS shows presence of carbonates and occluded sodium nitrate in the samples of the current study which contribute to weight loss.

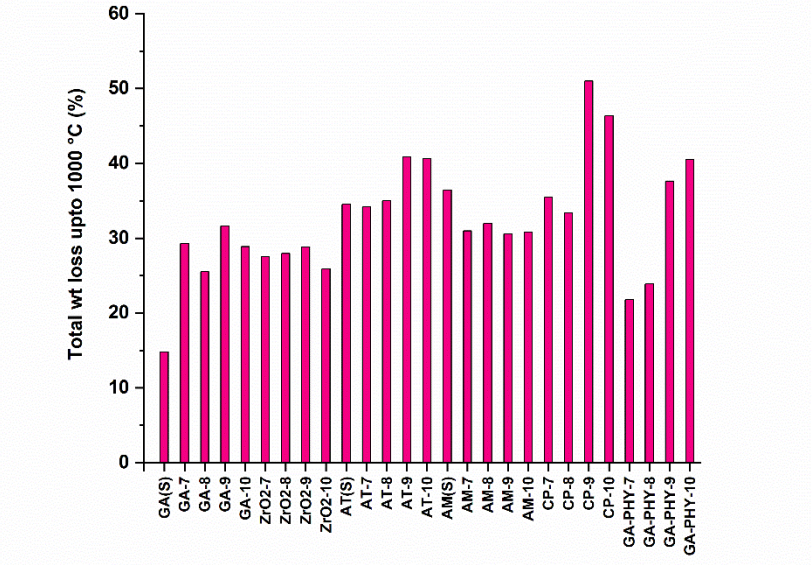

Figure 2. 12: %weight loss by TGA for different supports

From Figure 2.12 it is seen that, with respect to pH of precipitation, overall trend of total weight loss at pH 7-8 is AT≥ CP > AM > ZrO_2 ~ GA > GA-PHY whereas at pH 9-10 it is CP > AT > GA-PHY > AM ~ GA ~ ZrO_2. Indicating that different species are formed at these two ranges of pH. This is also confirmed from results of TGA-MS (Figures 2.14 and 2.15)

The following products are expected to form during precipitation: zirconium hydroxide, zirconium basic carbonate and sodium nitrate (by-product). Sodium zirconium hydroxyl or oxy carbonate is another possibility. Formation of amorphous aluminum hydroxycarbonate is reported from precipitation of aluminum nitrate with soda ash. It is stated to be non-stoichiometric with CO_3/Al = 0.5 max, where carbonate is directly coordinated to Al and also bound by electrostatic forces with sodium in the diffuse layer[41]. An unlikely possibility is presence of unreacted zirconium nitrate. Theoretical weight loss of these compounds are 22.6% (zirconium hydroxide), 59.7% (zirconium basic carbonate), 72.4% (zirconium nitrate hexahydrate) and 63% (Sodium nitrate). This was also confirmed by TGA analysis in the current work. The sodium zirconium hydroxyl or oxy carbonate is expected to give a weight loss in the range 40-56%[34][35]. Thus, weight loss exceeding 25-30% is indicative of presence of some of these compounds in addition to zirconium hydroxide in the as synthesized supports.

In order to understand the trends of TGA in a better manner, the weight loss was distributed across 4 ranges based on the phenomenon expected to occur based on results of TGA-MS (Figures 2.14 and 2.15).

1. Mainly loss of physisorbed water or water of crystallization/hydration at <200°C
2. Mainly dehydroxylation of alumina substrates and $Zr(OH)_4.xH_2O$ at 200-400°C along with some decarboxylation.
3. Mainly decarboxylation (as confirmed from evolved gas analysis) at 400-600°C along with some dehydroxylation
4. denitrification and decarboxylation at >600°C (as confirmed from evolved gas analysis).

The weight loss in these four regions was normalized on total weight loss (up to 1000°C).

Trend of normalized weight loss at <200°C, 200-400 °C, 400-600 °C and 600-800 °C is shown in Figure 2.13 a, b, c, d below.

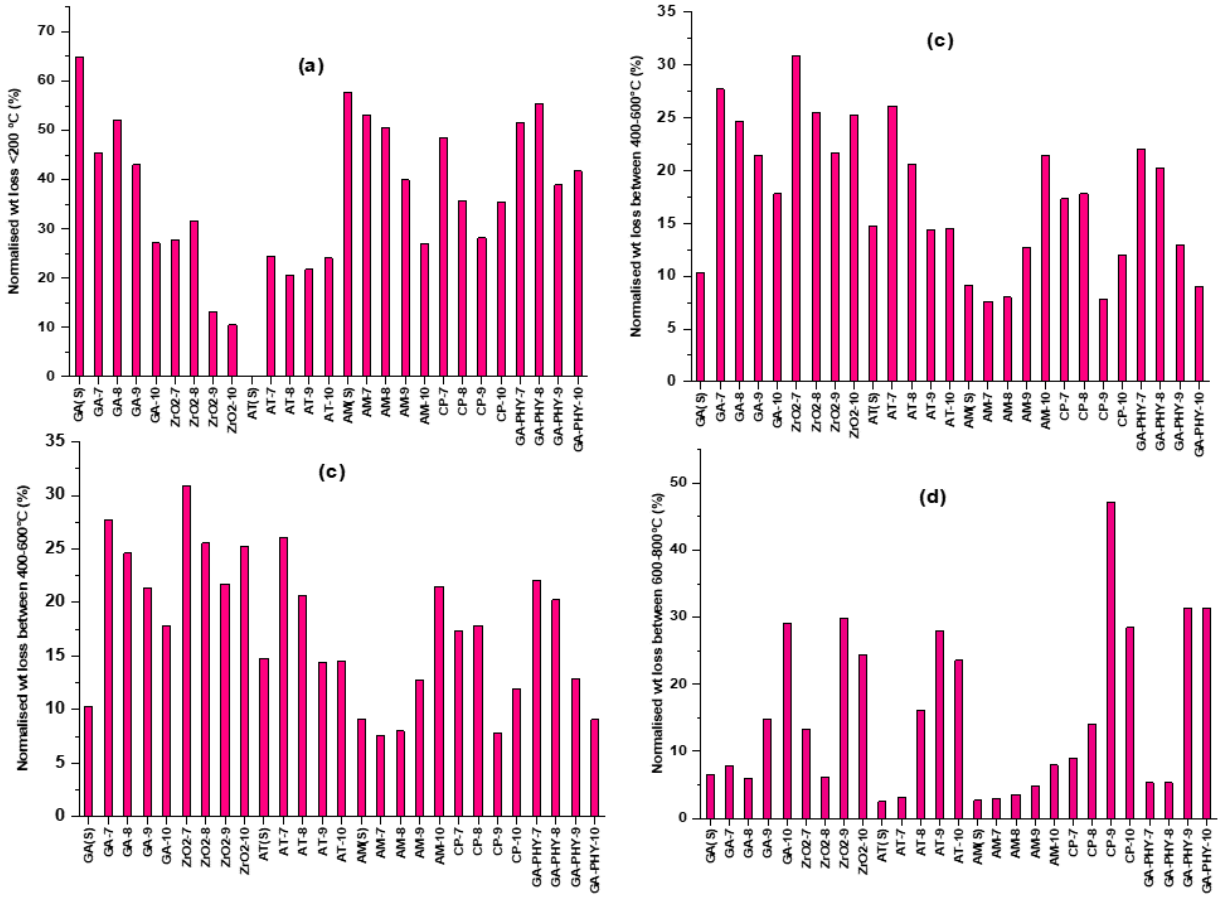

Figure 2. 13: Normalized wt loss (%) at (a) <200 °C (b) 200-400 °C (c) 400-600 °C and (d) 600-800 °C

Figure 2.13a shows the normalized weight loss of the supports at <200°C. As seen from this Figure the qualitative trend of weight loss for the bicomponent supports prepared by deposition-precipitation follows: AM ≥ GA-PHY ~ GA > AT. The weight loss of the substrates is also show in the Figure 2.13a. The significantly lower weigh loss of AT series is clearly due to absence of contribution from AT(S) substrate at this temperature. The weight loss in the AT series in this temperature range is solely due to loss from zirconium hydroxide/hydrated zirconia. The γ-Al_2O_3 (GA(S)) and pseudoboehmite (AM(S)) substrates show significant weight loss in this region. This trend also correlates with the decreasing order of the specific surface areas of the alumina substrates used to prepare them. This behavior is attributed to desorption of physisorbed water from GA(S) and AM(S) and dehydroxylation in case of AM(S). Physisorbed water is

expected to be proportional to specific surface area – GA(S) and AM(S) show high values, 250 and 300 m^2/g respectively.

Between supports prepared by precipitation i.e. ZrO_2 or co-precipitation (bi-component CP) the latter show higher weight loss. The specific surface area of the CP series is about $70m^2/g$ (for samples precipitated at pH 7-8) whereas it is <20 m^2/g for the ZrO_2 series. The higher weight loss of CP series is attributed to loss of physisorbed water from both the alumina and zirconia component and dehydroxylation of alumina component which is expected to be an oxyhydroxide of Al.

Figure 2.13b shows the normalized weight loss of the supports in the temperature range 200-400°C. The trend as seen from Figure 2.13b is AT ≥ AM > ZrO_2 > CP >GA = GA-PHY. For the solid alumina substrates used in deposition-precipitation, this trend matches with their degree of hydroxylation. AT(S) (which is a trihydroxide) is more hydroxylated than AM(S (which is an oxyhydroxide) which in turn is more hydroxylated than GA(S). AT(S) shows 82.5% of its total weight loss in this temperature range, thereby contributing to the high values. The AM-, ZrO_2- and GA- series show an increasing trend of weight loss with increasing pH of precipitation. Essentially, AT(S) and AM(S) substrates contribute to weight loss over and above that of $Zr(OH)_4.xH2O$ due to dehydroxylation. GA and GA-PHY series show lower weight loss because the GA(S) substrate is already dehydroxylated. TGA of GA(S) (Figure 2.8c) shows weak peaks in the 200-400°C region (2.7% weight loss), therefore the major contribution to weight loss in this region in GA and GA(PHY) series is solely from zirconia whose content is ~54 wt%. This explains the lower values. Considering that zirconia content is ~54%, the percentage weight loss 18-20% is in proportion to what is expected from $Zr(OH)_4.xH2O$. The CP series shows lower weight loss than AT and AM series as well as the ZrO_2 series. Hence they appear to be less hydroxylated. Al is trivalent and Zr tetravalent. Both are expected to form aquo, hydroxo or aquo-hydroxo species in solution over the entire pH scale studied. Thus both olation and oxolation can be expected to occur[42]. The former results in M-OH-M bridges whereas the latter results in M-O-M bridges. Based on lower weight loss in this region, the bi-component CP series appears to have undergone more oxolation than the mono-component ZrO_2 series. Formation of zirconia-alumina mixed oxides[43] is well known. Studies of Torres-Olea et.al.[43] report its formation with uniform distribution of Al and Zr in solids with 1:1 mole ratio. Oxolation is reported to occur over a wider range of pH than olation.

Olation is favored over oxolation for aquohydroxy precursors containing good aquo leaving groups. Zirconia is reported to undergo significant olation with increasing pH forming gelatinous precipitates[42]. The higher weight loss of ZrO_2 series relative to CP series is consistent with presence of more hydroxylated species in the former.

The trend of normalized weight loss in the 400-600°C segment is shown in Figure 2.13 c. All three substrates AT(S), GA(S) and AM(S) show some weight loss indicative of some dehydroxylation. The values are significantly lower than those of corresponding monocomponent zirconia (ZrO_2 series) or bicomponent supports. The reason for this is contribution from decarboxylation and denitrification in addition to dehydroxylation in case of the latter. As seen from Figure 2.13c, excepting for AM series which shows an increase in weight loss with increasing pH of precipitation, the remaining series all show a decrease in weight loss with increasing pH of precipitation. The difference is attributed to the relative ease of peptization of AM(S) substrate (which is a pseudoboehmite).

The trends in the temperature range 600-800°C are shown in Figure 2.13d. Comparing trend of weight loss at 400-600°C (Figures 2.13c) with 2.13d it is clear that the trend of Figure 2.13c is opposite that of Figure 2.13d. Percentage weight loss at 600-800°C increases with increasing pH of precipitation within a given series of supports in Figure 2.13d. Weight loss of samples precipitated at pH 9-10 is significantly higher than those which are precipitated at pH 7-8. The reason for this is clear from results of TGA-MS. The results of TGA-MS (Figures 2.14c for GA series and 2.15c for ZrO_2 series) clearly show presence of at least two species of metal carbonates, one which evolves CO_2 in the 400-600°C and the other which evolves it at 600-800°C. From peak positions of TGA-MS results it is observed that the concentration of the former is more in samples precipitated at pH 7-8 whereas the concentration of the latter is more in samples precipitated at pH 9-10. This explains the opposite trends of percentage weight loss in these two temperature regions. Further, evolution of some NOx is also observed in these samples (Figures 2.14d and 2.15d). The evolution of CO_2 is attributed to the decomposition of hydroxycarbonates and oxycarbonates of zirconium and the NOx to presence of occluded $NaNO_3$ which decomposes at these temperatures (as explained in section of evolved gas analysis).

As seen from Figures 2.13d all three substrates AT(S), AM(S) and GA(S) show low weight loss in the 600-800°C region, therefore the major contribution to weight loss in this region by the samples prepared by deposition-precipitation is mainly from (hydroxy)carbonates of zirconia and

occluded $NaNO_3$. Support CP-9 shows significantly higher weight loss than the remaining series. Reason for which is not clear.

In summary the trends of DSC-TG data clear point to differences in chemical moiety of the supports prepared using different substrates in deposition-precipitation and also by co-precipitation at the four different values of pH. Evolved gas analysis of select samples was carried out to identify the chemical species formed at different pH of preparation.

2.4.4.2 Evolved Gas Analysis (TGA-MS)

TGA-MS (evolved gas analysis) of select samples, GA and ZrO_2 series was done to identify the products of thermal decomposition. A mass spectrometer was coupled with the TGA. Results are given in Figures 2.14 and 2.15.

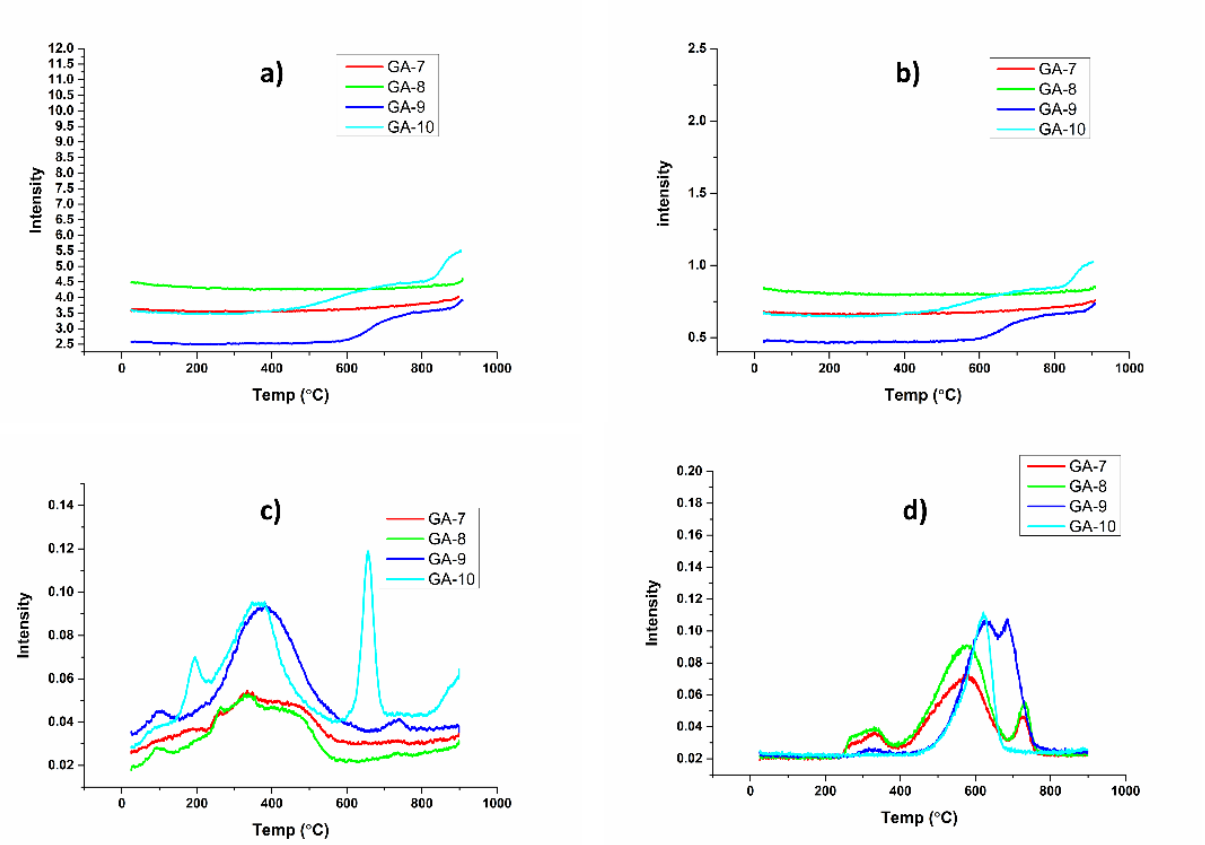

Figure 2. 14: Evolved gas analysis of GA series samples using TGA-MS (a) evolution of H_2O (m/z 18) (b) evolution of OH (m/z 17) (c) evolution of CO_2 (m/z 44) (d) evolution of NO (m/z 30)

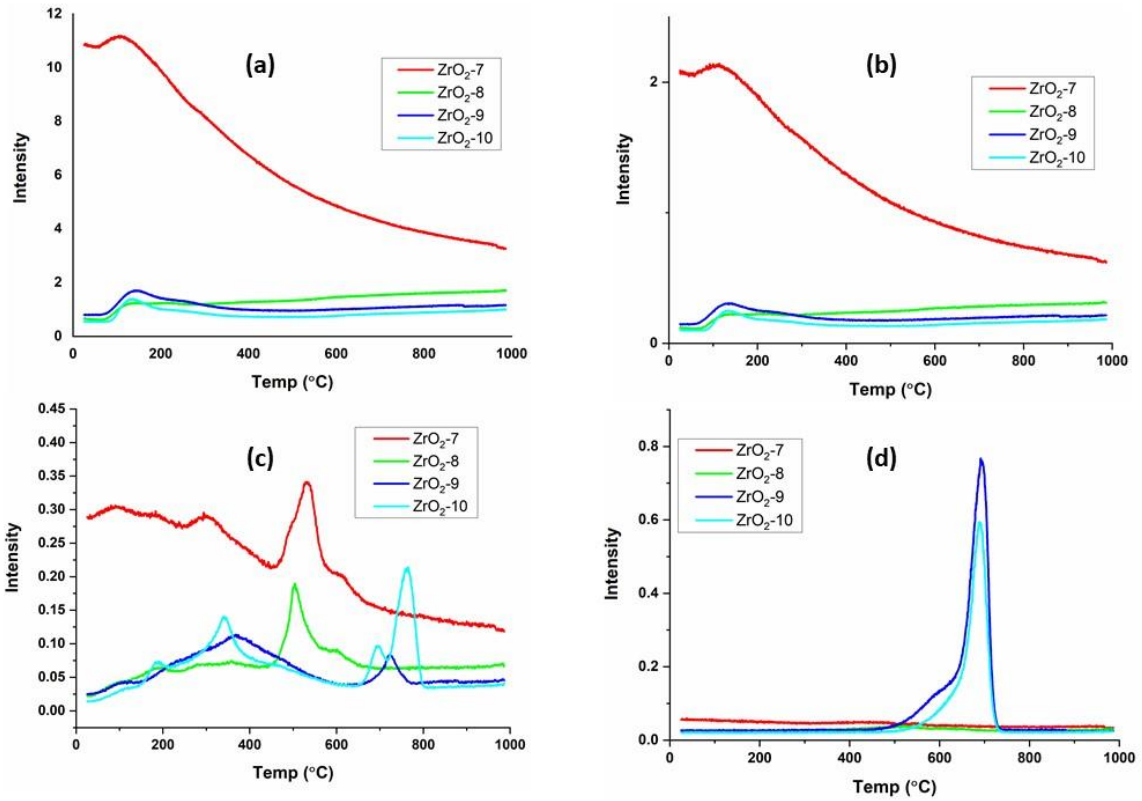

Figure 2. 15: Evolved gas analysis of ZrO2 series samples using TGA-MS (a) evolution of H2O (m/z 18) (b) evolution of OH (m/z 17) (c) evolution of CO_2 (m/z 44) (d) evolution of NO (m/z 30)

Based on identification of gases evolving during TGA-MS, loss of water from ZrO_2 is observed at temperature <200 °C (Figure 2.15a, 2.15b). Amongst the samples analyzed, loss of water and hydroxyls is maximum in support ZrO_2-7. This is supported by results of CHN and ICP-OES (Table 2.5) which show that supports prepared at pH 7 or 8 have higher hydroxide content.

Figure 2.15c shows that CO_2 is evolved in three distinctly different temperature ranges in the ZrO_2 series of supports. This indicates the presence of multiple carbonate species which undergo decarboxylation at 320-350°C, 500-530°C and 650-750°C. Results of FTIR (Figures 2.16 and 2.17) in subsequent sections confirm the presence of three different types of chelated metal carbonates which corroborate the existence of multiple carbonate species seen in evolved gas analysis by TGA-MS. Figure 2.14c (GA series) shows decarboxylation at 175°C, 350°C, 650°C and 750°C which are in the same temperature region as ZrO_2 series (Figure 2.15c). Comparison of Figure 2.14c with Figure 2.15c shows that decarboxylation in the lower temperature region

(~350°C) occurs as a broad peak in GA series whereas it occurs as sharp peaks (300-500°C range) in case of ZrO_2 series indicating some interaction between zirconia and alumina in GA series. In Figure 2.15c (TGA-MS of ZrO_2 series) zirconium (hydroxy)carbonate species decompose with sharp peaks at about 325, 500°C, 700°C and 750°C. Both water and CO_2 are evolved. The high temperature peaks at 650-800°C (Figure 2.13c) are absent in samples prepared at pH ≤8. Carbonate decomposition is endothermic which is clearly seen from DSC figures in Figure 2.9b. The high temperature peaks for decarboxylation in the current study compare well with studies of preparation of nano zirconia from ammonium zirconium carbonate by Rubio et.al[44]. Rubio et. al. report the endothermic decomposition of carbonate in the temperature range 650-700°C.

NO evolved in TGA-MS of all the GA and ZrO_2 samples (Figure 2.14d and 2.15d) indicating the presence of compounds containing nitrate. The nitrates mainly decompose at 550-575°C in samples of GA series which are prepared at pH 7 and 8 with a minor evolution at 725°C (Figure 2.14d). The maxima of this peak moves to higher temperature (600-700°C) when pH of precipitation is increased to 9 or 10. The ZrO_2 samples (Figure 2.15d) precipitated at pH 7-8 do not show peaks in the 550-575°C region. While those precipitated at pH 9-10 show a sharp peak at about 670-700°C with a small ascending shoulder at about 570°C. D. Laing et al.[45] have reviewed published literature on the thermal decomposition behavior of Sodium nitrate. They report that nitrite is formed during this process and it decomposes at temperature >700°C releasing NOx. NO evolves in the same temperature range in the current study (as reported by Liang et.al.). DSC-TG of pure basic zirconium nitrate showed peaks at 120°C and 232°C. The latter peak is attributed to the decomposition of the nitrate. Thus, the presence of unreacted nitrate of zirconium in the bicomponent supports prepared in this work is unlikely.

2.4.5 FTIR

The as synthesized dried samples of GA-series of supports (with γ-Al_2O_3 as the substrate) were subjected to FTIR to identify the species of carbonate and correlate them with their decarboxylation at the three different temperatures as seen in TGA-MS studies. Figure 2.16 shows the results of FTIR in transmission mode for this set of samples. The structure of different types of metal-carbonate species which are reported in literature is shown in Figure 2.17.

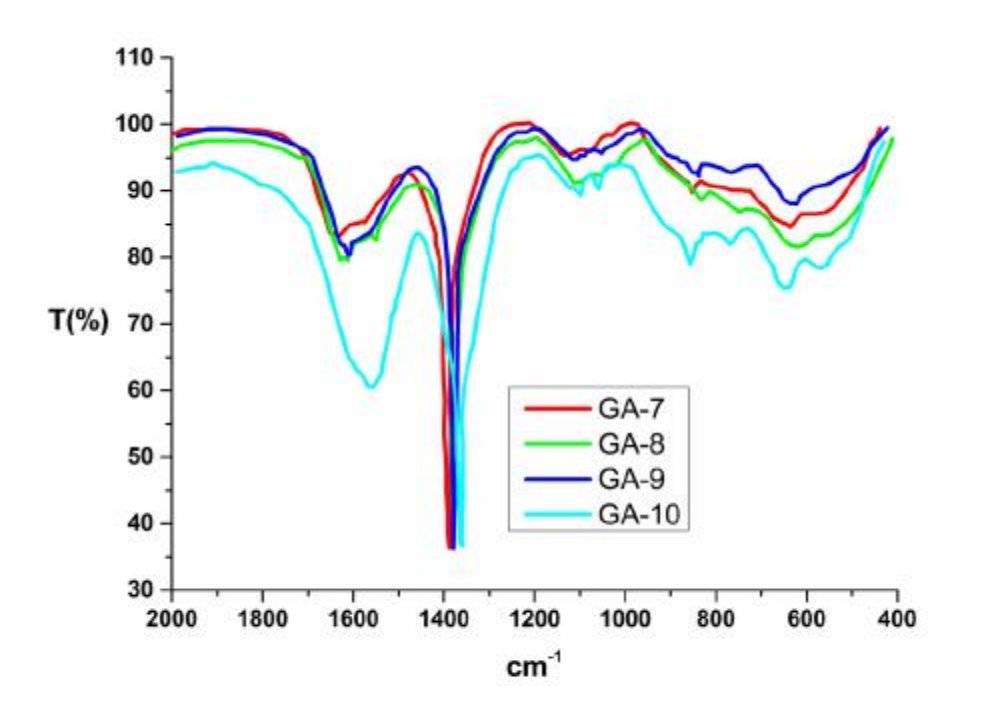

Figure 2. 16: various types of metal-carbonate species based on FTIR.

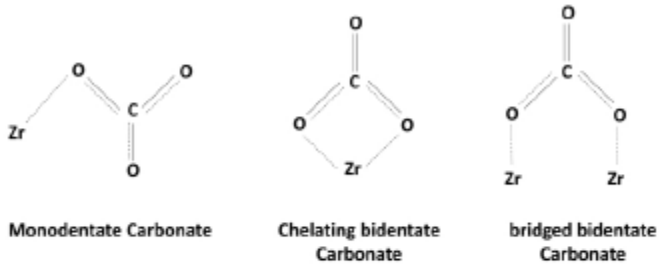

Figure 2. 17: Carbonate species in different co-ordination with metal ion

A peak at about 3440 cm^{-1} was observed in all the samples. This peak is attributed to hydroxyls (not shown in Figure 2.16). The structure of monodentate metal carbonate is shown in Figure 2.17. Based on literature references[46][47] this species of carbonate shows a peak at about 1384 cm^{-1}. This peak is observed in all the samples studied. Bridged bidentate metal carbonate is reported to show peaks in the 1620-1633 cm^{-1} region. These peaks are also observed at this wave number in samples prepared at pH-7 and pH-8. They progressively shift to lower wave number with an increase in the pH of preparation of samples. GA-9 which is prepared at pH 9 shows this

peak at 1618 cm^{-1} whereas GA-10 which is prepared at pH 10 shows this peak at 1574 cm^{-1}. The bands in GA-7 and GA-8 are attributed to bridged bidentate metal carbonate while those of GA-9 and GA-10 are assigned to chelating bidentate metal carbonate based on the same literature references.

Thus, it is evident that the type of metal carbonate species formed changes with pH of preparation. A clear distinction is observed for samples prepared at pH ≤8 and those prepared at pH >8. These results corroborate with those of TGA-MS studies (Figures 2.14c and 2.15c) which show that CO_2 evolves in three different temperature ranges. The samples prepared at pH >8 show exceptional stability in the decomposition of MBOH which is covered in subsequent section of this chapter.

2.4.6 CHN analysis

In order to quantify the carbonates and nitrates observed in evolved gas analysis, CHN analysis of GA and ZrO_2 series of supports was carried out to understand composition of neat zirconia and bicomponent zirconia-alumina. Results are provided in Table 2.4.

Support	C (wt. %)	H (wt. %)	N (wt. %)
GA-7	1.13	1.99	0.99
GA-8	1.89	1.98	1.01
GA-9	2.43	1.96	1.76
GA-10	3.54	1.61	1.26
ZrO_2-7	2.7	1.39	1.3
ZrO_2-8	3.32	1.18	1.2
ZrO_2-9	3.8	1.19	1.6
ZrO_2-10	4.58	1.22	2

Table 2. 4: CHN analysis of GA and ZrO_2 series

Results of CHN analysis of the GA-# and ZrO_2-# series of supports which are dried at 120°C are presented in Table 2.4. They confirm the presence of carbon, hydrogen and nitrogen in these samples. CO_2 is expected to evolve by decarboxylation of the carbonate species, Nitrogen

from denitrification of nitrate species and hydrogen (as water) from dehydroxylation. The carbon and nitrogen contents increase with increase in pH of precipitation in both sets viz. GA and ZrO_2 series of supports.

Based on zirconia content determined from ICP-OES, and carbon, hydrogen and nitrogen from CHN analysis, the fraction of zirconium existing as the carbonate or the hydroxide was calculated. The fractional moles of Zr computed as its carbonate or its hydroxide are presented in Table 2.5. The mole ratios of NO_3:Na are also included in the Table.

	Mole fraction of Na present as nitrate and Zr present as carbonate or hydroxide			
Support	**NO_3/Na**	**Mole fraction of Zr as its carbonate**	**Mole fraction of Zr as its hydroxide**	**Total Moles of Zr**
GA-7	1.06	0.11	1.17	1.280
GA-8	1.01	0.186	1.14	1.326
GA-9	0.99	0.239	1.16	1.399
GA-10	1.03	0.342	0.93	1.272
GA-PHY-7	0.98	0.226	0.62	0.846
GA-PHY-10	1.02	0.374	0.76	1.134
ZrO_2-7	0.97	0.237	0.733	0.970
ZrO_2-8	1.05	0.312	0.666	0.979
ZrO_2-9	1.01	0.339	0.637	0.976
ZrO_2-10	0.99	0.371	0.592	0.963

Table 2. 5: Molar fraction of zirconium as carbonate and hydroxide and molar ratio of NO3:Na derived from combined results of ICP-OES, Flame photometry and CHN analysis

The following stoichiometric equations were used to calculate the mole fractions of Zr as its carbonate and its hydroxide.

$$Zr(NO_3)_4 + 2Na_2CO_3 = Zr(CO_3)_2 + 4NaNO_3 \qquad \textit{Equation 4}$$

$$Zr(NO_3)_4 + 4NaOH = Zr(OH)_4 + 4NaNO_3 \qquad \text{Equation 5}$$

The NaOH is formed through anion hydrolysis of CO_3^{2-} by the reaction

$$2\,Na+ + CO_3^{2-} + 2\,H_2O = 2\,Na+ + 2\,OH^- + H_2CO_3 \qquad \text{Equation 6}$$

The moles of carbonate, hydroxide and nitrate were calculated from the moles of C, H and N determined from CHN analysis. The zirconium content of samples was obtained from results of ICP-OES analysis and the Na content from Flame photometry for samples dried at 120°C. As seen from Table 2.5 relatively more zirconium hydroxide than zirconium carbonate forms when the pH of precipitation is ≤8. The trend reverses when pH of precipitation is >8. In the samples of neat zirconia (ZrO_2 series) 0.24 to 0.37 mole fraction of the zirconium exists in the form of its carbonate. Also the carbonate fraction increases with increasing pH of preparation. About 0.60 to 0.73 mole fraction of the Zr exists as the hydroxide. These two fractions account for 0.96-0.98 mole fraction of the zirconium in the ZrO_2 series which is a good tally.

Based on the above results the typical/generic composition of these supports can be expressed as.

$$0.45\,Al_2O_3\ 0.53\,Zr\,(CO_3)_a\,(OH)_b\ 0.02\,NaNO_3 \qquad \text{Equation 7}$$

where a varies from 0.27-0.41 and b from 0.59-0.73

In the case of the bi-component GA series which are prepared by deposition-precipitation the hydroxide fraction exceeds 1.0, thus the sum total of fraction of Zr computed as the carbonate and the hydroxide exceeds 1.0. This is due to contribution from water associated with the alumina component which contributes to the H content determined from CHN analysis in the GA series.
In the case of the bi-component GA-PHY series (GA-PHY-7 and GA-PHY-10) the total of fractions of Zr computed as its carbonate and its hydroxide present values of 0.84 and 1.13 respectively. The wide variation is attributed to inhomogeneity of local composition of these samples. Results of EDAX of these samples which are presented in Table 2.3 support this argument.

The molar ratio of NO_3:Na as determined from the N in CHN analysis and Na as determined by Flame photometry are also shown in Table 2.5. The values range from 0.97 to 1.06 which is close to the stoichiometric value of 1.0. This indicates that the sodium and nitrate exist in the form of $NaNO_3$ in all the samples.

The values of CO_3/Zr of the above samples fall in the same range as reported in the following published literature. Basic zirconium carbonate with molecular formula $Zr(OH)_2CO_3.ZrO_2$ (CAS 57219-64-4) or values reported in European patent EP 0004403 B1[48] ($Na_AZr_BCO_{3C}$) or US patent number 6627164B1[49][35] as $NaZrO_2CO_3.nH_2O$, or as $Na_4[ZrOZr(OH)_2(CO_3)_4].8H_2O$ (various forms of sodium zirconium hydroxycarbonate)[34]. Thus, the results of the current study show that the zirconium in the supports of the current study exists as combinations of its hydroxide and carbonate.

2.4.7 X-ray Diffraction

2.4.7.1 XRD of 120 °C dried supports

XRD diffractograms of substrates are shown in Figure 2.18 a, b, c below.

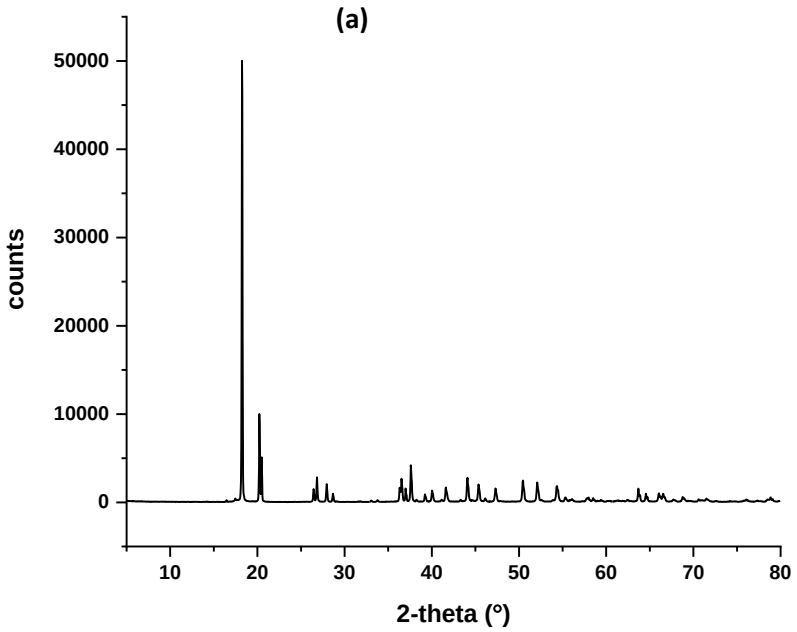

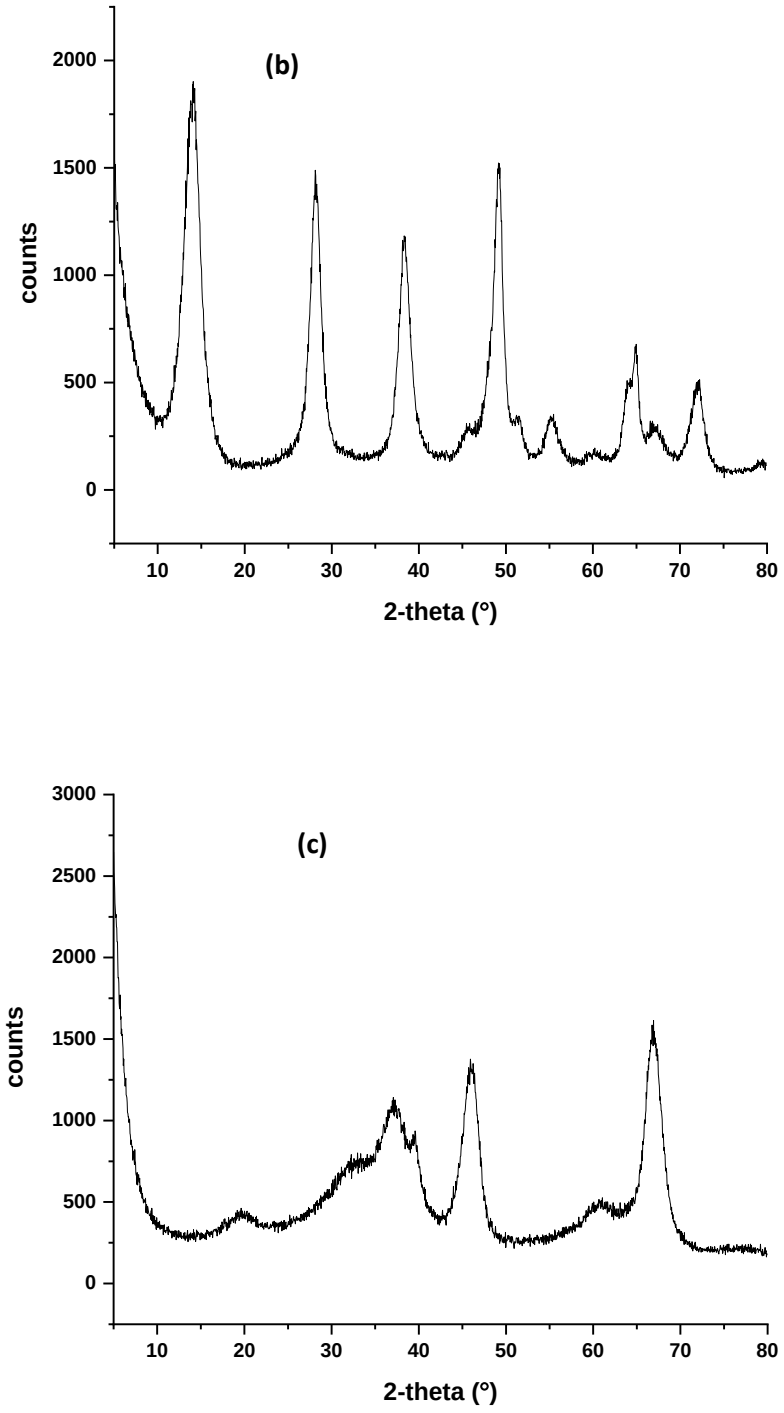

Figure 2. 18: XRD of alumina substrates used for deposition-precipitation (a) AT(S) (b) AM(S) (c) GA(S)

As seen from Figure 2.18, AT(S) shows high crystallinity. Both AM(S) and GA(S) are quazi-crystalline when compared to AT(S). There is a clear difference in peak positions and intensities between peaks of all three AT(S), AM(S) and GA(S).

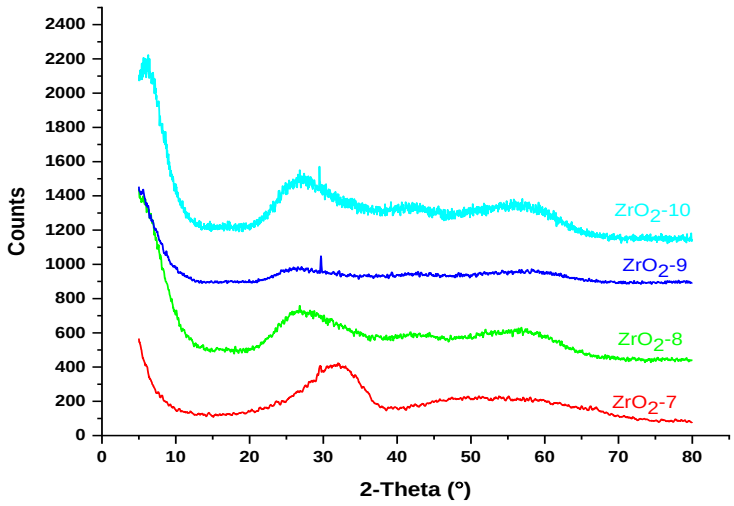

Figure 2. 19: XRD of ZrO_2 Series

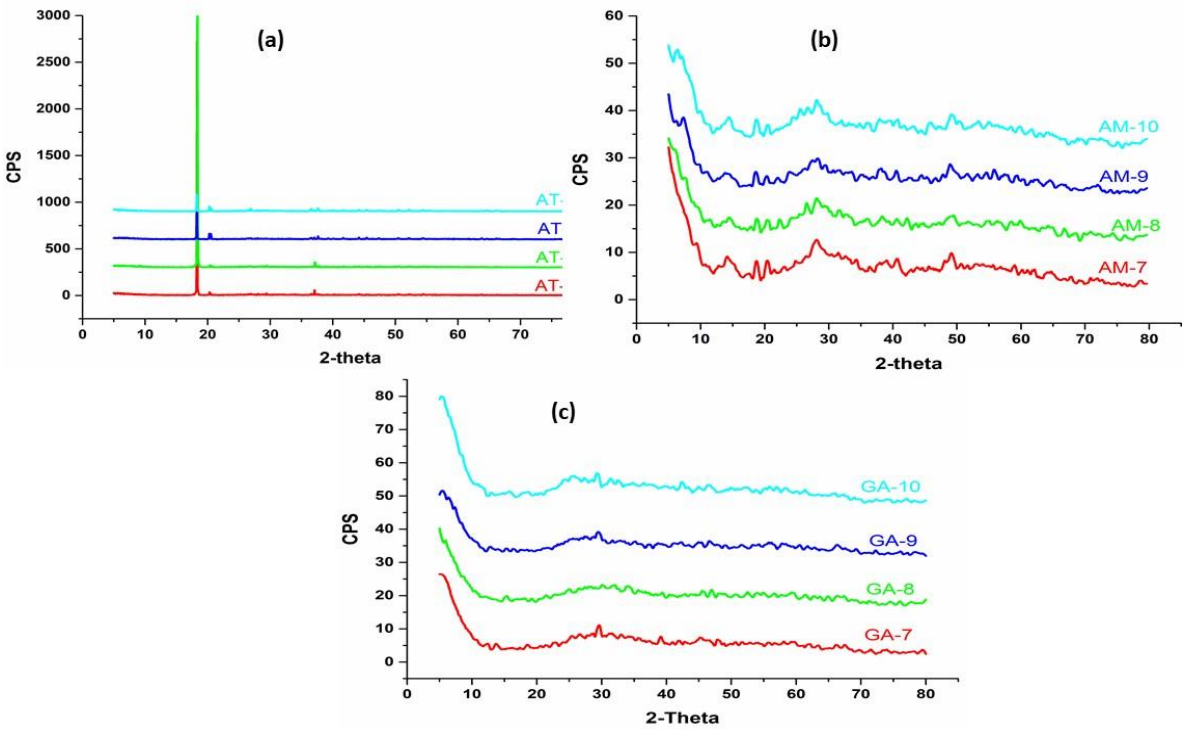

Figure 2. 20: XRD of supports prepared by deposition-precipitation using different alumina substrates (a) AT series (b) AM series (c) GA series

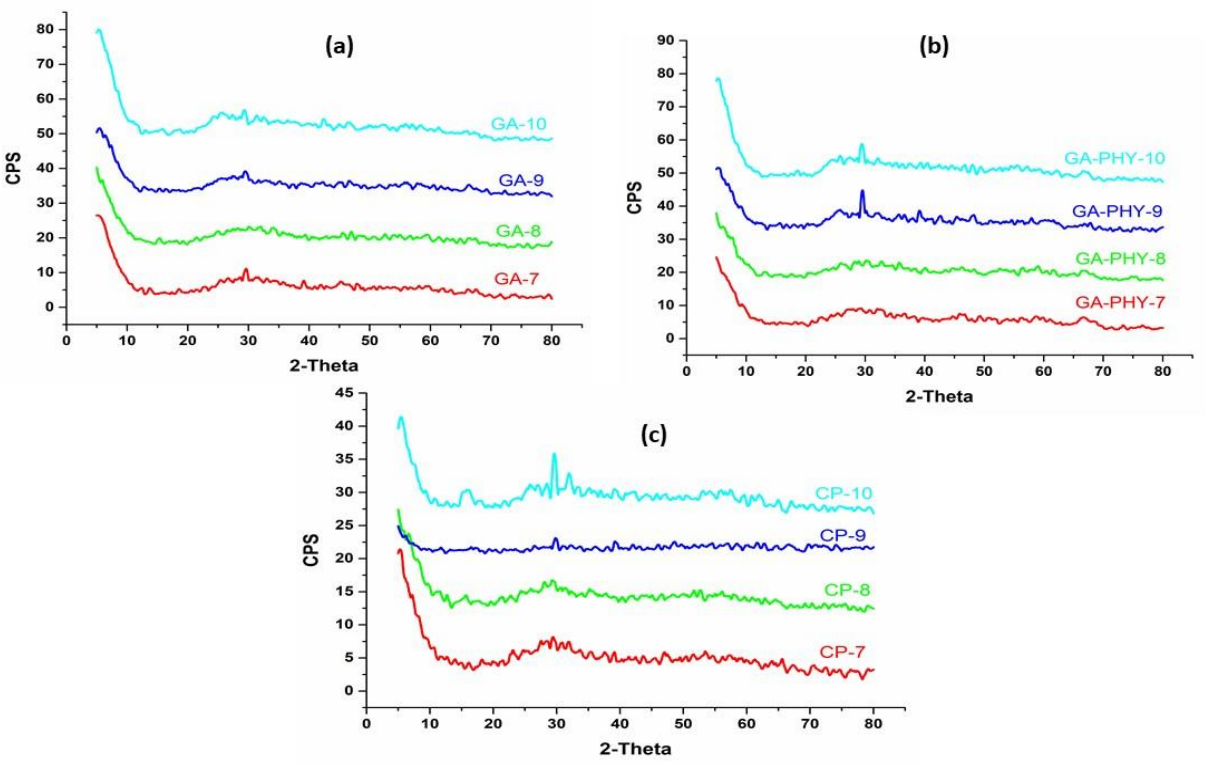

Figure 2. 21: XRD of supports prepared by different methods (a) GA series – Deposition-Precipitation method (b) GA-PHY series – Physical Mixing method (c) CP series – co-precipitation method

XRD diffractograms of the as synthesized bicomponent zirconia-alumina supports prepared by deposition-precipitation using the three substrates AT(S), AM(S) and GA(S) are presented in Figure 2.20 a,b,c above. XRD diffractogram of ZrO_2 series is shown in Figure 2.19 above. XRD diffractograms of GA, GA-PHY and CP series are shown in Figure 2.21 above. All these samples are dried at 120°C. As seen from Figures 2.19, 2.20 and 2.21 the materials are largely X-ray amorphous in nature which is expected because they are only dried at 120°C. Stichert and Schuth[30] have prepared precipitated zirconia using $ZrOCl_2.8H_2O$ and NH_4OH at pH 10±0.2, followed by washing and drying at 90°C. The concentration of zirconium salt was also varied in their studies. As per their results XRD of samples which are prepared using zirconium salt with

molar concentration <0.06 M and which are calcined at ≤350°C present amorphous phase. In the present study, an aqueous solution of zirconium nitrate 0.068M and 2.5 M aqueous sodium carbonate were used as reagents. The XRD results are similar to those obtained in the study by Stichert et.al. and Davis et al[30][28]. Davis et.al. have studied the effect of pH on precipitated zirconia materials where zirconia gel was precipitated from zirconyl nitrate solution (0.6 M) by rapidly adding aqueous ammonia (7 wt%) in pH range 3 to 14. The precipitate was washed with distilled water and dried in air at 110°C. Through substitution of aqueous ammonia with solutions of alkali hydroxides, they have further determined that the presence of alkali, calcination atmosphere and temperature history during calcination do not play a dominant role on the crystallinity of the resultant samples. These studies indicate that the zirconia gel formed has a similar structure when it is precipitated in the pH range 6.5 to 10.4.[28] In the present work, samples were prepared in pH range 7 to 10 with sodium carbonate as precipitant Significant differences were seen in composition (hydroxide: carbonate) and metal-carbonate structure (FTIR and CHN studies). Subtle differences in acidity (by MBOH model reaction) and significantly slower deactivation was observed between samples precipitate at pH ≤8 or >8. Kurapova et al.[29] have reviewed studies on phase evolution of zirconia based systems. They have reported the work of Santos et al.[50] wherein the equivalence point for titration of precipitation of an acid solution of a zirconium salt with base is reported to occur at pH 9. The precipitation of $Zr(OH)_4$ is stated to take place at a pH just after 9. Based on results of weight loss in TGA of the current study, zirconia is present as $Zr(OH)_4.xH_2O$ rather than $ZrO_2.xH_2O$ which is consistent with work of Santos et.al.

The most intense XRD peak of Na_2O is at 2θ 29.5°. This peak is observed in most of the samples of GA-PHY, GA and CP series (Figures 2.21). It was not seen in samples of AT series (Figure 2.20a) due to much higher intensity of aluminum trihydrate peak 2θ ~18.2° which masks the Na_2O peak, however presence of Na_2O in AT series is clearly observed in chemical analysis. It is also not visible in GA-PHY-7, GA-PHY-8 (Figure 2.21 b), GA-8 (Figure 2.20 c), and all of the AM series of supports (Figure 2.20 b). It is probably X-ray amorphous in these latter samples. Figure 2.20a shows the X-ray diffractogram of the AT series. The peak at 2θ 18.2° is characteristic of aluminum trihydrate. The intensity of this peak decreases with increasing pH of preparation but all peaks characteristic of AT(S) are clearly present in good intensity indicating that AT(S) does not undergo significant change under preparation conditions of deposition-precipitation. Figure 2.20 b shows X-ray diffractogram of the supports of AM series. Peaks characteristic of

pseudoboehmite at 14.2, 28.0 and 49.3° are seen as very small diffused peaks. The intensity of pseudoboehmite peaks relative to the AM(S) substrate (Figure 2.18 b) are significantly diminished indicating that it has undergone significant change under preparation conditions of deposition-precipitation. Na_2O was not detected in XRD of AM series, but identified in ICP-OES analysis. Hence it exists as X-ray amorphous phase. The X-ray diffractogram of GA series is shown in Figure 2.20c. Presence of Na_2O is evident in these supports. Peak of the γ-phase is observed as small diffused broad peak (67.03° 2-theta). The intensity of this peak relative to the GA(S) substrate (Figure 2.18c) is significantly diminished indicating that it has undergone significant change under preparation conditions of deposition-precipitation.

Figures 2.21b shows the X-ray diffractogram of the GA-PHY series of supports. Peak for Na_2O at 29.5° 2θ is observed in samples GA-PHY-9 and GA-PHY-10. The peak of γ-Al_2O_3 at 2-θ 67.0°is visible as a small peak. It is more prominent than in GA(#) supports. Figure 2.21 c shows the X-ray diffractogram of the CP series of supports which are prepared by co-precipitation. Presence of Na_2O is clearly seen in sample CP-10 and to a lesser extent in sample CP-9. The remaining peaks are diffused and broad (amorphous nature). The pattern is largely similar to that of AM(S) and GA(S) series with a broad peak at about 30° 2θ. Peaks of t-ZrO_2 which is expected at 2-theta 30.182° is not seen in any of the samples including that of the ZrO_2-series of supports

2.4.7.2 XRD of calcined supports

XRD pattern of the above supports calcined at 550°C 8h is shown below in Figures 2.22 a) GA-series b) ZrO_2 series, c) AM-series d) CP series. Suffix Cal is used after the name of the sample. All the calcined supports (Figure 2.22) show zirconia in its tetragonal form. Kurapova et al.[29] have also cited the work of B.G. Linsen [51] wherein NaOH is used to precipitate zirconia from $ZrOCl.8H_2O$ at pH 4, 6 and 8, it is reported that acidic medium favors formation of monoclinic zirconia after calcination whereas metastable t-ZrO_2 is formed when the precipitation is carried out in alkaline condition. All the supports of the present study were prepared in pH range 7-10. The results are consistent with those of Linsen et.al., the samples show t-ZrO_2 phase.

Samples of GA, ZrO_2, AM and CP series prepared at the two extremes of pH (7 and 10) were calcined at 550°C for 8h. Their XRD pattern is shown in Figure 2.22 a, b, c and d. After calcination all eight samples show presence of tetragonal zirconia (t-ZrO_2) by XRD. Supports

ZrO_2-7Cal and ZrO_2-10Cal (Figure 2.22 b) show all four peaks of t-ZrO_2. The crystallite size decreases when pH of precipitation is increased from 7 to 10 (Table 2.6). In supports GA-7Cal and GA-10Cal (zirconia deposited on γ-Al_2O_3, Figure 2.22 a,), the most intense peak of gamma alumina which is expected at 2Θ of 66.72° is practically absent. Further, the most intense peak of zirconia at 2θ 30.182°, which is sharp in the ZrO_2-Cal series (Figure 2.22 b) becomes less intense, broad and diffused when zirconia is supported on GA(S) (Figure 2.22 a). The second most intense peak of ZrO_2 at 2θ 35.034° (Figure 2.22 b) practically disappears in Figures 2.22 a, b while the intensity of peaks at 50.43° and 59.97° decreases substantially. Thus, thermal crystallization of zirconia is inhibited when it is deposited on γ-Al_2O_3, which indicates strong interaction between zirconia and γ-alumina at their interface. The change in peak intensity is more in GA-7Cal than in GA-10Cal indicating relatively more acid peptization of the γ-Al_2O_3 substrate at preparation conditions of GA-7. Kirsch et.al[52]have reported that when tetragonal and amorphous hydrous zirconia colloids are coated with alumina (precipitated from its propoxide) the temperature for crystallization from amorphous to tetragonal zirconia increases from 600°C to 1050°C. A similar effect is observed in the current studies when 50 mole% zirconia is deposited on the surface of γ-Al_2O_3 from its nitrate salt solution. The crystallization of amorphous zirconia is suppressed at 550°C.

The XRD patterns of AM-7Cal and AM-10Cal and CP-7Cal and CP-10Cal series which are calcined at 550°C 8h are shown in Figure 2.22c and 2.22d respectively. As seen from Figure 2.22c, peaks of t-ZrO_2 are significantly subdued in AM-7(Cal). Excepting for the most intense peak at 30.182° 2-theta, the remaining peaks are practically not visible. However, there is a significant increase in intensity of all four XRD peaks of zirconia in AM-10Cal (where pH of precipitation is increased from 7 to 10). Peak of gamma alumina at 2Θ of 66.72° is clearly seen in both supports indicating phase transformation of alumina. A similar behavior is observed for the calcined supports CP-7Cal and CP-10Cal (Figure 2.22d). Intensity of XRD peaks of t-zirconia is significantly subdued in AM-7Cal and CP-7Cal which are prepared at pH 7 which indicates strong interaction and inhibition of thermal crystallization of zirconia when compared to the AM-10Cal and CP-10Cal supports which are prepared at pH 10. Morikawa et.al.[53] have proposed concept of diffusion barrier wherein alumina acts as a barrier which inhibits sintering of ceria-zirconia. Therein, they have co-precipitated ceria, zirconia and alumina to form a solid solution. Their

studies show that the presence of alumina inhibits sintering of ceria zirconia. Similar inhibition of sintering is observed in the AM-7Cal and CP-7Cal zirconia-alumina composites of the current study. The Al is present in a chemically reactive form in both these cases. As oxyhydroxide/pseudoboehmite (in AM-series) and as a cation (Al^{3+}) in CP-series. Strong interaction between the two components retards crystallization of zirconia and the composites (AM-7Cal and CP-7Cal) tend to remain as largely amorphous materials upon calcination at 550°C. However, in supports AM-10Cal and CP-10Cal (which are prepared at final pH 10), zirconia appears to segregate from the solid solution and crystallize as its tetragonal phase during calcination. Cause for segregation is attributed to a combined effect of a) difference in carbonate and nitrate species when the support is prepared at pH 7-8 or pH 9-10 (as seen from results of TGA-MS, Figures 2.12 and 2.13) and b) thermal phase transition of the alumina precursors. Such thermal phase transition of alumina does not take place in the GA(#) series where the alumina substrate is already in the γ-form which is significantly less chemically reactive. The role of anions in stabilizing t-ZrO_2 is reviewed at length by S. Shukla and S. Seal[54]. The presence of anions is reported to stabilize t-ZrO_2 by modifying surface energies and thus prevent formation of the m-ZrO_2 phase, which is otherwise expected to form.

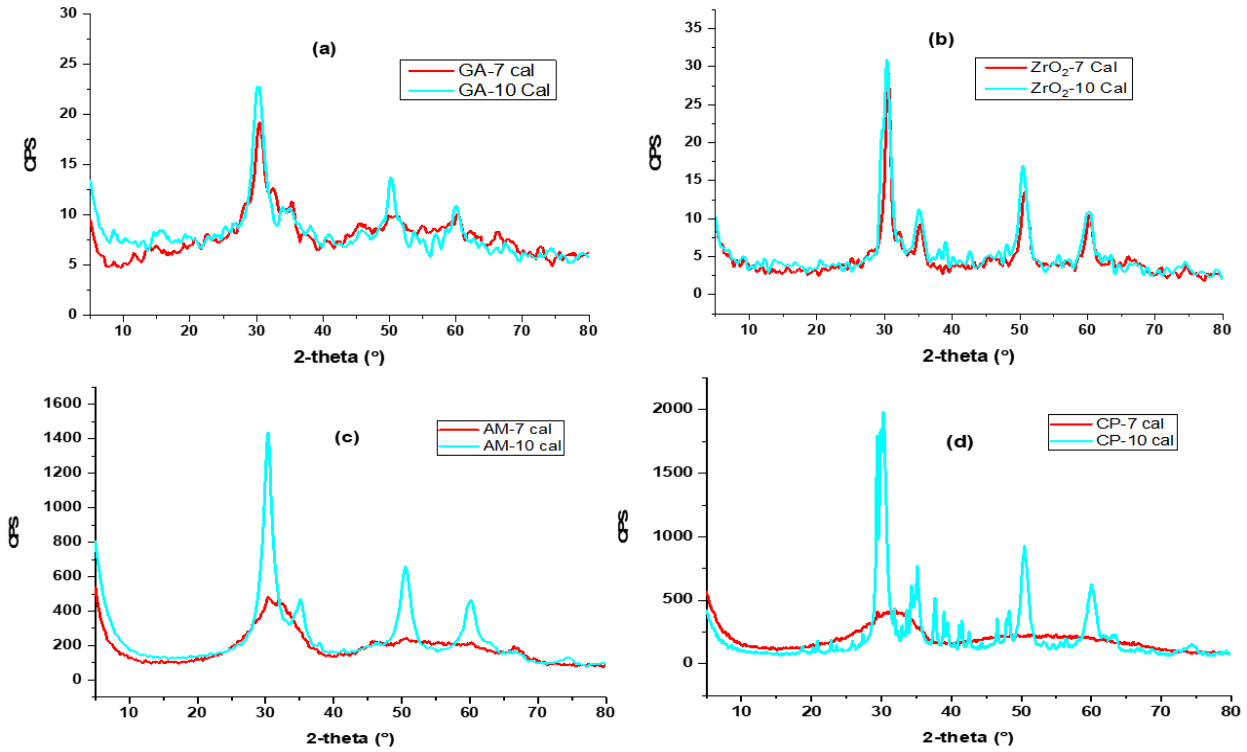

Figure 2. 22: X-ray diffractogram of (a) GA-7, GA-10, (b) ZrO_2-7, ZrO_2-10, c) AM-7, AM-10 and d) CP-7 and CP-10 supports calcined at 550℃ 8h

The reactive nature of Al precursors used in preparation of the AM and CP series also reflects in their drastic loss of pore volume and average pore diameter (in AM-series) in comparison to the GA-series of supports. This renders the AM(S) unsuitable as a support for preparation of bicomponent supports by deposition precipitation. The surface area (Figure 2.3) and pore volume (Figure 2.4) of the CP-series of supports is also about half of that of the GA-series (Figures 2.3 and 2.4) which is a disadvantage.

The studies of Kurapova et.al. [29] show that an acidic medium of precipitation favors formation of m-ZrO_2 whereas a basic medium favors formation of t-ZrO_2. The results of the current study are in agreement with those of Kurupova et.al. However, Davis[28], has reported that zirconia precipitated at pH between 6.5-10.4 is predominantly monoclinic. The results of the current study are contrary to those of Davis et.al. A review of published literature suggests that different parameters of preparation like crystal size formed during the step of precipitation[30], conditions of aging of the precipitate in its mother liquor[55], and a combination of different preparation parameters such as pH, temperature and aging[56] etc. influence the phase of zirconia formed upon calcination. Jerome Chevalier et.al.[57] report that the phase transformation of t-ZrO_2 to m-ZrO_2 also depends on whether moisture is present or absent during calcination. The above aspects need to be taken into account for interpreting the phase formation of zirconia. A dry atmosphere (without added moisture) was used for calcination of the samples in the current study which could explain the formation of t-ZrO_2. Thus, the difference in phase with respect to results of Davis et.al. is attributed to differences in the above parameters.

The crystallite size of zirconia in the calcined catalysts was calculated from the Scherrer equation for the peak at 2Θ 30.182° (for t-ZrO_2). Values for the bicomponent zirconia-alumina samples GA-7Cal, GA-10Cal, AM-7Cal and AM-10Cal prepared by deposition-precipitation, ZrO_2-7Cal and ZrO_2-10Cal prepared by strike precipitation and CP-7Cal and CP-10Cal prepared by co-precipitation are presented in Table 2.6 below. These samples were calcined at 550°C, 8h.

Supports	pH of precipitation	Crystallite size (Å)
GA-7Cal	7	55
GA-10Cal	10	43
ZrO_2-7Cal	7	94
ZrO_2-10Cal	10	61
AM-7Cal	7	11
AM-10Cal	10	51.7
CP-7Cal	7	14
CP-10Cal	10	70

Table 2. 6: Crystallite size of GA-7 Cal, GA-10 Cal, ZrO_2-7 Cal, ZrO_2-10 Cal, AM-7 Cal, AM-10 Cal, CP-7 Cal and CP-10 Cal

It is observed from Table 2.6 that crystallite size decreases when pH of preparation is increased from 7 to 10 in the calcined ZrO_2 and GA-series of supports. Whereas the AM and CP series of supports show an opposite trend, crystallite size increases with pH in these cases. Overall, the crystallite size of supports prepared by both deposition-precipitation and co-precipitation are lower than that of neat zirconia (ZrO_2) at a given pH of preparation. CP-10Cal is an exception. The reason for the difference between the GA series and the AM / CP series appears to be the relatively inert form of Al substrate/precursor used in preparation of the former series versus the chemically reactive form of Al precursor in the latter two series. This is already explained in detail in an earlier section. The significantly smaller crystallite size of zirconia in AM-7Cal and CP-7Cal is attractive, however consequences are loss of specific surface area (Figure 2.3) and pore volume (Figure 2.4) of these materials which is a clear disadvantage. Higher pH at elevated temperature (60°C) facilitates dissolution and re-precipitation which could result in improved dispersion, hence smaller crystallite size can be expected. Studies carried out by Carter et.al.[58] show that the crystallite size of calcined samples of zirconia depends on the pH of precipitation. It is smaller

when the samples are precipitated at pH 12 than at pH 3. Data at intermediate pH is not available in their studies. The results of GA and ZrO2 series are directionally in agreement with their results. Overall the GA-series (γ-Al_2O_3 substrate) has advantages both from good interaction with zirconia which minimizes sintering as well as good specific surface area, pore volume and average pore diameter at the higher pH of precipitation.

2.4.8 Scanning Electron Microscopy

SEM of select samples of the as prepared supports of GA, ZrO_2 and CP series was carried out to understand effect of pH on morphology.

SEM of as synthesized samples of GA, ZrO_2 and CP series are shown in Figures 2.23, 2.24 and 2.25 below respectively.

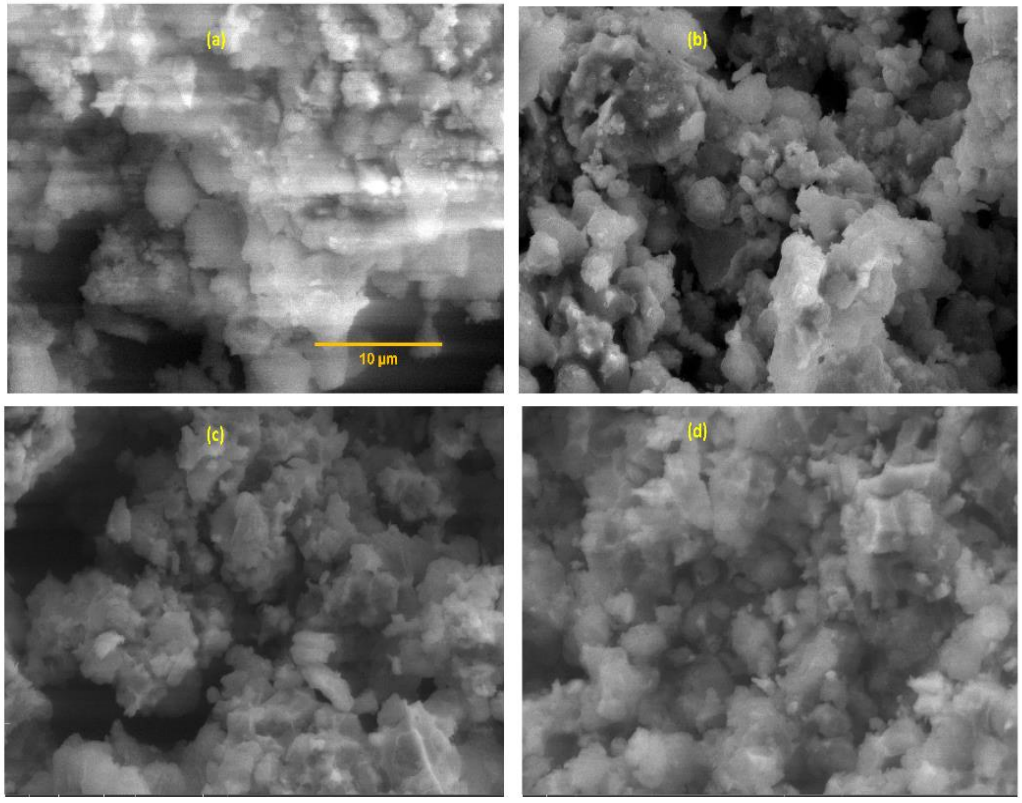

Figure 2. 23: SEM images of (a) GA-7 (b) GA-8 (c) GA-9 and (d) GA-10

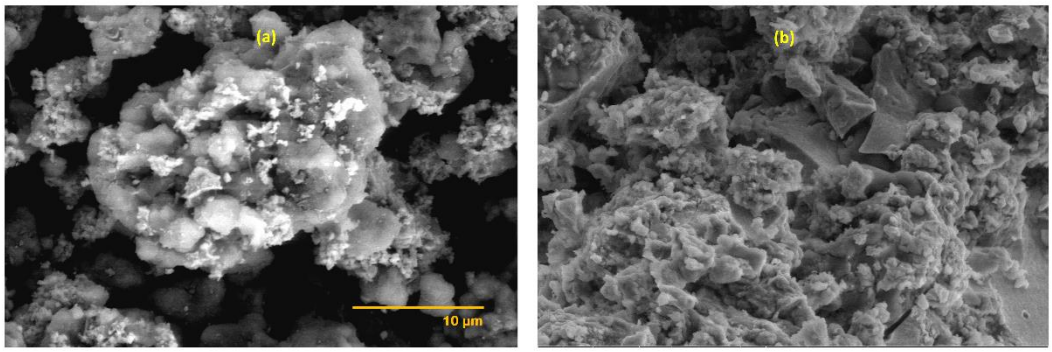

Figure 2. 24: SEM images of (a)ZrO_2-7 (b) ZrO_2-10

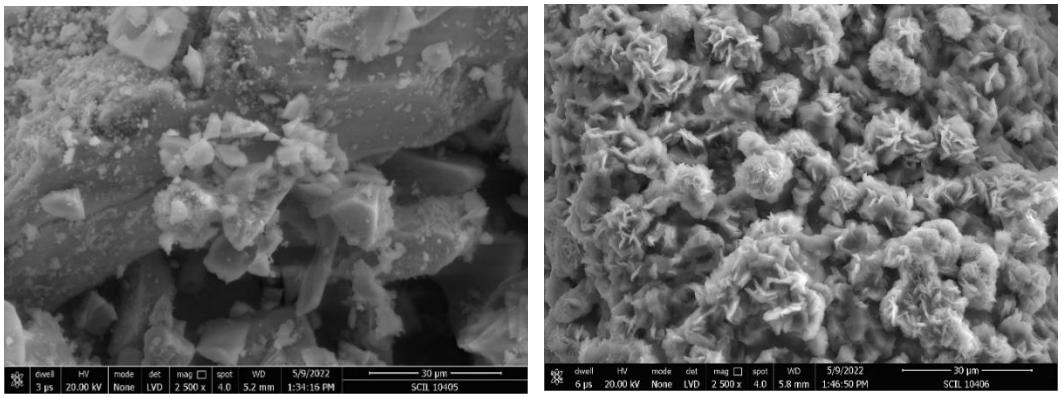

Figure 2. 25 : SEM images of (a)CP-7 (b)CP-10

As seen from Figure 2.23 a, GA-7 shows irregular granular morphology. This morphology transitions to a smaller size of granules and a flaky texture when the pH of precipitation increases (Figures 2.23 b, c, d). A higher degree of homogeneity is also observed. However, this is at an expense of textural properties. Both surface and pore volume decrease drastically with increasing pH of precipitation. As regards samples of neat zirconia, while sample ZrO_2-7 (Figure 2.24 a) shows clumps of globules consisting of both small and large particles with attendant voids, sample ZrO_2-10 (Figure 2.24 b) shows a texture reminiscent of dried gel structure which has low porosity. The ZrO2 series shows poor textural properties irrespective of the pH of precipitation. Comparing the GA series (Figure 2.23, which are prepared by deposition-precipitation) with ZrO_2 series (Figure 2.24 a, b which are prepared by strike precipitation) it is observed that the ZrO2 series shows a relatively more granular morphology. The supports prepared by co-precipitation at pH 7

(sample CP-7, Figure 2.25 a) show morphology which is blocky (block-like). This explains its relatively lower specific surface area when compared to GA-7 which is prepared by deposition precipitation at the same pH. CP-10 which is prepared by coprecipitation at pH 10 (Figure 2.25 b) shows a distinctly different flower-like morphology consisting of a combination of dense fibers and platelets. Morphology of CP-# series is relatively closer to that of ZrO_2-# series than GA-# series. However, the surface area of this sample (CP-10) is very low (4-5 m^2/g).

Overall, SEM images indicate that deposition-precipitation facilitates dispersion of zirconia on the alumina substrate and improves surface area of zirconia particles, as also seen from results of N_2 physisorption (Figure 2.3).

2.5 MBOH model test reaction (Acidic, basic and amphoteric sites):

The decomposition of MBOH (2-methyl-3butyn-2-ol) is reported to proceed by three parallel pathways. It is converted to equimolar quantities of acetone and acetylene on basic sites, to 3-methyl-3-buten-1yne (MByne) or Prenal (3-methylcrotonaldehyde) on acidic sites or 3-hydroxy-3-methyl-butanone (HMB) and 3-methyl-3-buten-2-one (MiPk) over amphoteric sites[59].

Conversion of MBOH of all the samples at the 1st hour on stream is shown in Figure 2.26 below. The conversion of MBOH on neat substrate materials is shown immediately prior to the respective series of bi-component supports which are prepared using that substrate.

All the samples of neat substrate materials used in this study, AT(S), AM(S) and GA(S) show >98% conversion at the first hour on stream. The neat zirconia samples ZrO_2-7 and ZrO_2-10 too show high conversion >95%.

Most of the bi-component support samples which are prepared by deposition-precipitation show high initial conversion typically >98.6% regardless of the substrate used or the pH of precipitation in their preparation. AT-7 and AT-8 which showed lower conversion 93.4 and 67.6%, respectively, are exceptions. There is no visible trend of conversion at first hour on stream with respect to pH of precipitation for any of the other series of supports which are prepared by deposition-precipitation.

2.5.1 Conversion of MBOH

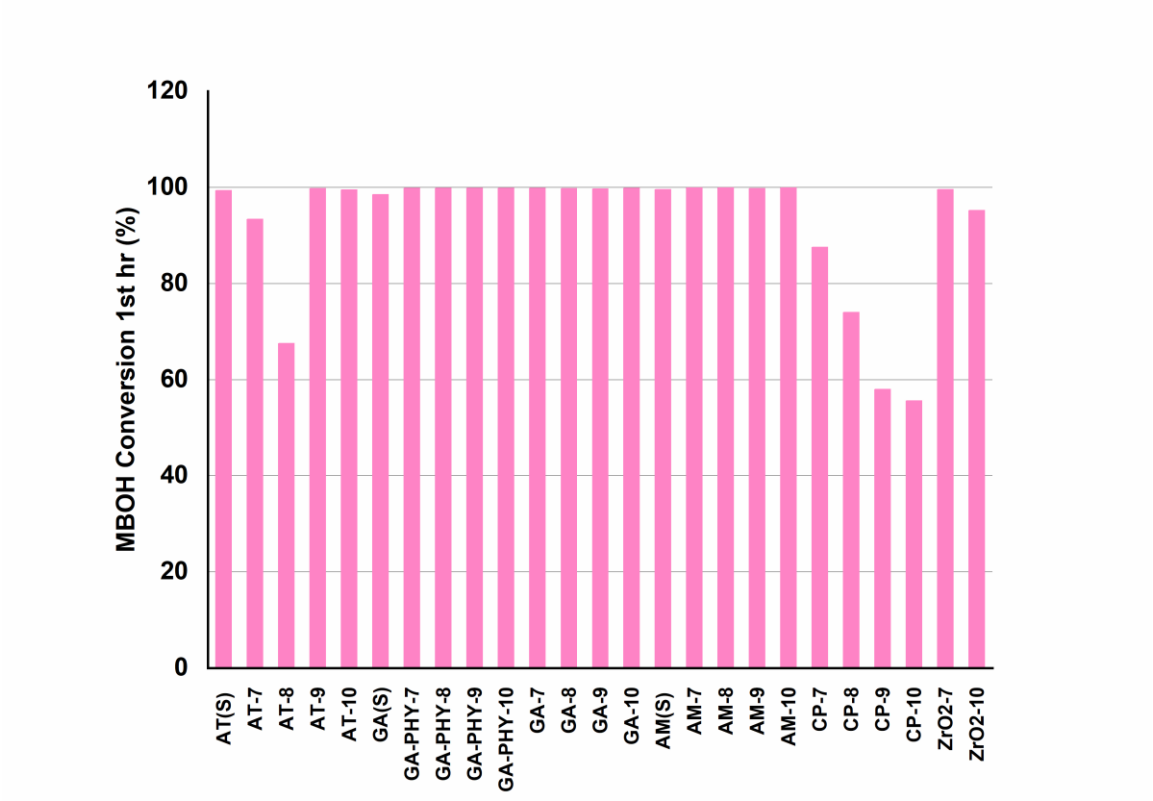

Figure 2. 26: Comparison of conversion of MBOH of different supports at the first hour on stream

The CP series of supports which were prepared by co-precipitation show significantly lower conversion (55.6-87.5%) at the first hour on stream than the supports which are prepared by deposition-precipitation. This holds over the entire range of pH of preparation (7-10). This series (CP) shows a trend of decrease in conversion at the 1st hour on stream with increasing pH of preparation. It is interesting to note that samples with widely different specific surface area ZrO_2 (14-17 m^2/g) and AT series (11-25 m^2/g) GA(S) and AM(S) (250 and 300 m^2/g respectively) give initial conversions >98%. Thus, the lower activity of AT-7, AT-8 or the entire CP series (~75 m^2/g for samples prepared at pH <8 and 4-5 m2/g for samples prepared at pH >8) cannot be attributed to their low specific surface area. The reactivity appears to be largely inherent to the chemical character of these samples rather than their specific surface area.

All the bi-component samples which are prepared at pH 9 and 10 have a significantly lower specific surface area and pore volume than those prepared at pH 7 or 8 (Figures 2.3, 2.4

respectively), yet they show high conversion at first hour on stream >99.5%. Results of evolved gas analysis by TGA-MS (Figures 2.14 and 2.15) and FTIR (Figure 2.16) have shown that significantly different chemical species are formed when final pH of precipitation is 9 or 10. Arithmetic means of conversion averaged over 8 hours on stream and normalized for specific BET surface area of the support sample are shown in Figure 2.27.

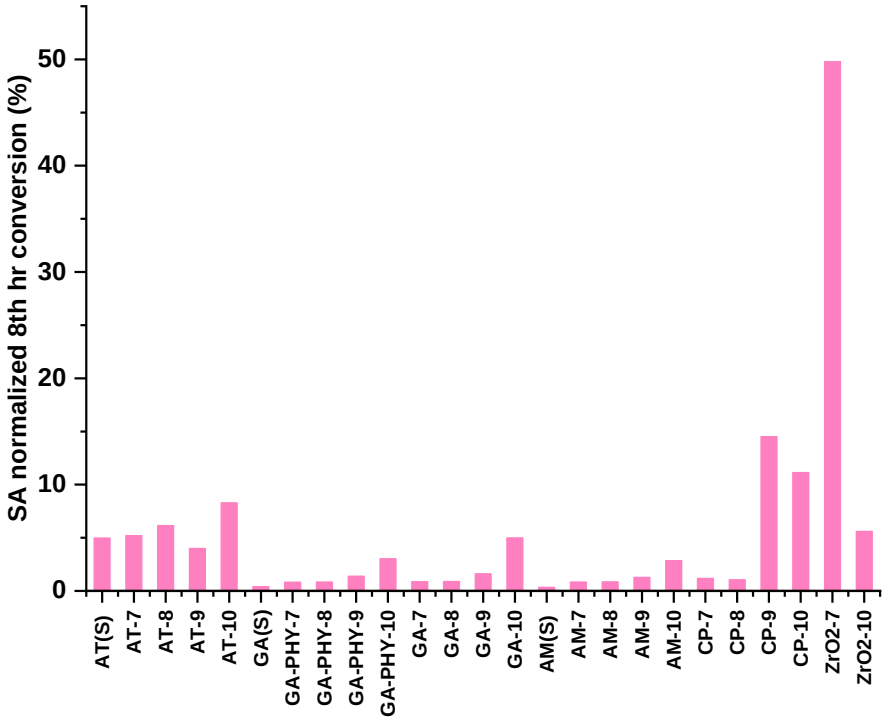

Figure 2. 27: Average of conversion over 8 hours on stream normalized for specific BET surface area

As seen from Figure 2.27, the values of conversion which are normalized for specific BET surface area show an increasing trend with pH of preparation for all the series of supports irrespective of the method of preparation and also irrespective of the substrate used in the case of supports prepared by deposition-precipitation. These results indicate that the chemical species of zirconia formed in samples which are prepared at pH 9 and 10 are significantly different and more active and stable for the conversion of MBOH than support samples which are prepared at final pH 7 and 8. As noted from XRD studies (Table 2.6) the crystallite size of zirconia decreases with increasing pH of precipitation. Smaller crystallite size results in higher dispersion which is beneficial for activity and can influence product selectivity. The results of evolved gas analysis

using TGA-MS (Figures 2.14 and 2.15) indicate that different species of carbonate and nitrate are formed when supports are prepared at pH 9 or 10. Likewise results of FTIR (Figure 2.16) also show differences in metal carbonate species when pH is increased to 9 or 10. These results support the above presumption.

2.5.2 Selectivity of acetone (Basic sites)

Figure 2.28 shows the selectivity to acetone (and acetylene) for the different samples. Selectivity for this is higher than 90% for all the samples. Thus, all the samples show predominantly basic character. The selectivity to acetylene is not shown in Figure 2.28, however it forms in nearly equimolar quantities to that of acetone. Lauron-Pernot et al.[31] have studied the influence of sodium content in alumina on reactivity for MBOH. Their results show that increasing sodium content lends basic character to the oxide. Concentration of sodium oxide greater than 4 wt% is reported to completely subdue acidic and amphoteric character of alumina in their studies. The results in current study are largely consistent with the study of Lauron-Pernot et al., in that the samples display basic character. However, some residual acidic and amphoteric character is still present. This is attributed to differences in the materials and reaction conditions. The materials of the present study are bicomponent zirconia-alumina and the reaction temperature is significantly higher (240°C) versus 180°C in the work of Lauron-Pernot. It is interesting that some acidic and amphoteric character (see Figures 2.29-2.31) is observed in spite of the significant content of sodium in these samples.

From Figure 2.28 it is observed that amongst the neat substrates trend for basicity is AT(S)>AM(S)>GA(S). This is consistent with the observation that AT(S) (Gibbsite) forms CHI alumina whereas AM(S) (pseudoboehmite) forms γ-Al_2O_3 upon calcination through dehydroxylation. γ-Al_2O_3 is known for its high acidity amongst transition aluminas[37]. Both the samples of neat zirconia, viz. ZrO_2-7 and ZrO_2-10 which are precipitated at final pH 7 and 10 respectively, show strong basic character hence, all the bi-component supports which are produced by deposition-precipitation produce significantly higher acetone than the neat substrates themselves.

Figure 2. 28: Trends of selectivity for formation of acetone

A possible reason for a predominantly basic character could be the significant amount of Na_2O which remained behind in the samples in spite of washing with hot demineralized water. Lauron-Pernot et al.[31] have studied the influence of sodium content in alumina on reactivity for MBOH. Their results show that increasing sodium content lends basic character to the oxide. Concentration of sodium oxide greater than 4 wt% is reported to completely subdue acidic and amphoteric character of alumina in their studies. In order to understand the effect of Na_2O on catalytic behavior, sample ZrO_2-10 was washed extensively to decrease its soda content to ~500 ppm and was tested for the MBOH reaction. The results of soda content, conversion at the 1st hour on stream and selectivity to different products of this sample is compared with the results of samples ZrO_2-7 and ZrO_2-10 as such i.e without additional washing in Table 2.7. Results show that removing soda by washing has a relatively small effect on conversion.

Sample	Na_2O (wt%)	Conversion (%) at 1st hour	MByne (%)	Acetone (%)	MiPk (%)	HMB (%)	Carbon (%)
ZrO_2-7	4.2	99.6	5.0	90.4	2.0	0	3.2
ZrO_2-10	6.3	95.3	1.4	97.1	0.03	0.08	1.6
ZrO_2-10 (washed)	0.05	98.0	1.9	85.6	1.9	9.1	2.3

Table 2. 7: Comparison of reactivity of neat zirconium carbonate with different Na_2O content

However, product selectivity shifts from basic towards amphoteric behavior when Na_2O of the sample ZrO_2-10 is removed by extensive washing. The selectivity to HMB and MiPk increase significantly at the expense of acetone. Tomishige et al.[60] have attributed acid-base pairs of zirconia to its amphoteric nature. Studies of Lauron-Pernot et al.[31] also show that ZrO_2 has predominant amphoteric character in its reactivity to MBOH. Results of the current study show an increase in amphoteric character when the sodium content is decreased by washing, however, the sample still shows predominantly basic character. ZrO_2-7 which is prepared at pH 7 and has 4.2 wt% Na_2O produces significantly higher amounts of MByne (which is indicative of acidity) compared to ZrO_2-10, even after soda is decreased significantly in the latter sample by washing. Thus, the selectivity trends observed in the case of the bi-component support samples prepared by deposition-precipitation in this work appears to be due to the inherent difference in chemical moiety of these samples (which in turn is dependent on pH).

2.5.3 Selectivity of MByne (Acidic sites)

Subtle differences in amphoteric and acidic sites were also observed in the present study. Figure 2.29 shows product selectivity to MByne. Selectivity of alumina substrates to MByne are presented separately in Table 2.8 because they show significantly higher selectivity to this product and it is unwieldy to plot on the same graph.

Sample	Selectivity of MByne (%)	Selectivity of Acetone (%)	Selectivity of MiPk (%)	Selectivity of HMB (%)	Carbon (%)
AT(S)	5.4	92.6	1.1	0.13	1.4
AM(S)	20.2	68.3	8.4	0	3.6
GA(S)	34	47	14	0.06	5.0

Table 2. 8: Product selectivity of MBOH decomposition over substrate materials

From the results in Table 2.8 above, the trend of the acid character of the substrate materials which is characterized by the formation of MByne is GA(S) > AM(S) >> AT(S), is the exact opposite of trend for basicity. From Figure 2.29 it is seen that, within a given series which are prepared by deposition-precipitation with a specific substrate, selectivity to MByne decreases as the pH of preparation is increased from 7 to 10. Neat ZrO_2 samples also show this trend. CP series supports do not show a definite trend in this respect. Sample AT-8 (of the AT series) shows unusually high selectivity for MByne amongst these samples. The reason for this different behavior is not clear. The acid character of all the three aluminum oxide based substrates is largely suppressed, and only some residual acid character is observed in the bicomponent support samples, which is attributed to the presence of occluded soda.

Amongst the bicomponent series, AT and CP show relatively higher selectivity to MByne than the AM or GA series. It is interesting that although AT(S) substrate shows lower acidity than the AM(S) or GA(S) substrates, its bi-component supports show higher acidity similar to unsupported zirconia (ZrO_2 series). This is attributed to the lower surface area and higher bulk density of AT(S) which presents lower geometric surface area for deposition of zirconia. Thus, this series is expected to have poor dispersion of zirconia relative to the AM and GA series, which explains its behavior like unsupported ZrO_2. The relatively higher acidity of the CP series is attributed to formation of zirconia-alumina mixed oxides[61].

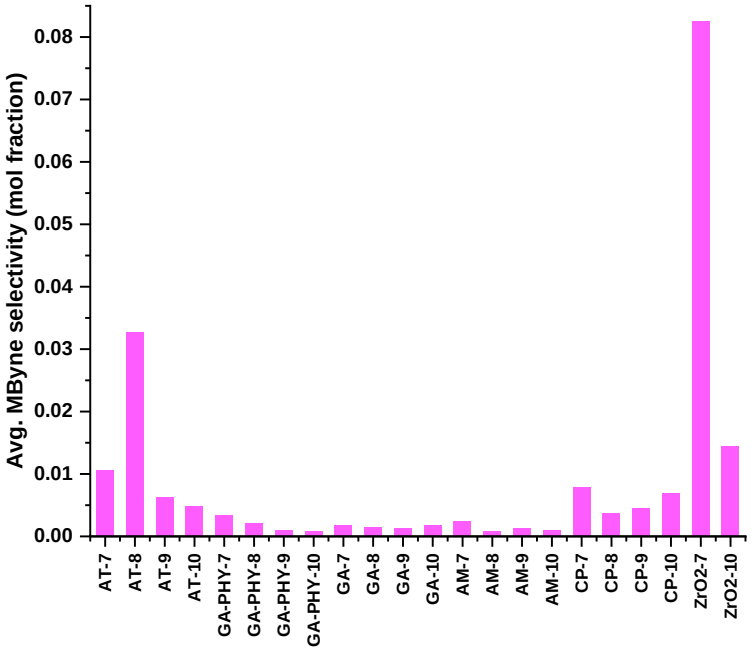

Figure 2. 29: Trends of selectivity for formation of MByne

2.5.4 Selectivity of HMB and MiPk (Amphoteric sites)

Figure 2.30 shows selectivity of HMB for neat substrates as well as for supports. Amongst the neat substrates GA(S) shows relatively higher selectivity to HMB than AM(S) and AT(S). The mono-component zirconia materials ZrO_2-7, ZrO_2-10 show low selectivity to HMB.

Within the series of supports prepared by deposition-precipitation with a specific substrate, samples prepared at pH 7 and 8 show higher selectivity to HMB. Again, there is no clear trend in case of the CP series which are prepared by co-precipitation. Between the series of bi-component support samples trend for formation of HMB is AT > AM > GA-PHY > GA series when they are prepared at pH ≤8. Supports prepared by physical mixing (GA-PHY series) show higher HMB formation than their counterparts GA series which are prepared by deposition-precipitation. This is attributed to lesser extent of interaction between the zirconia and alumina phases in case of the former.

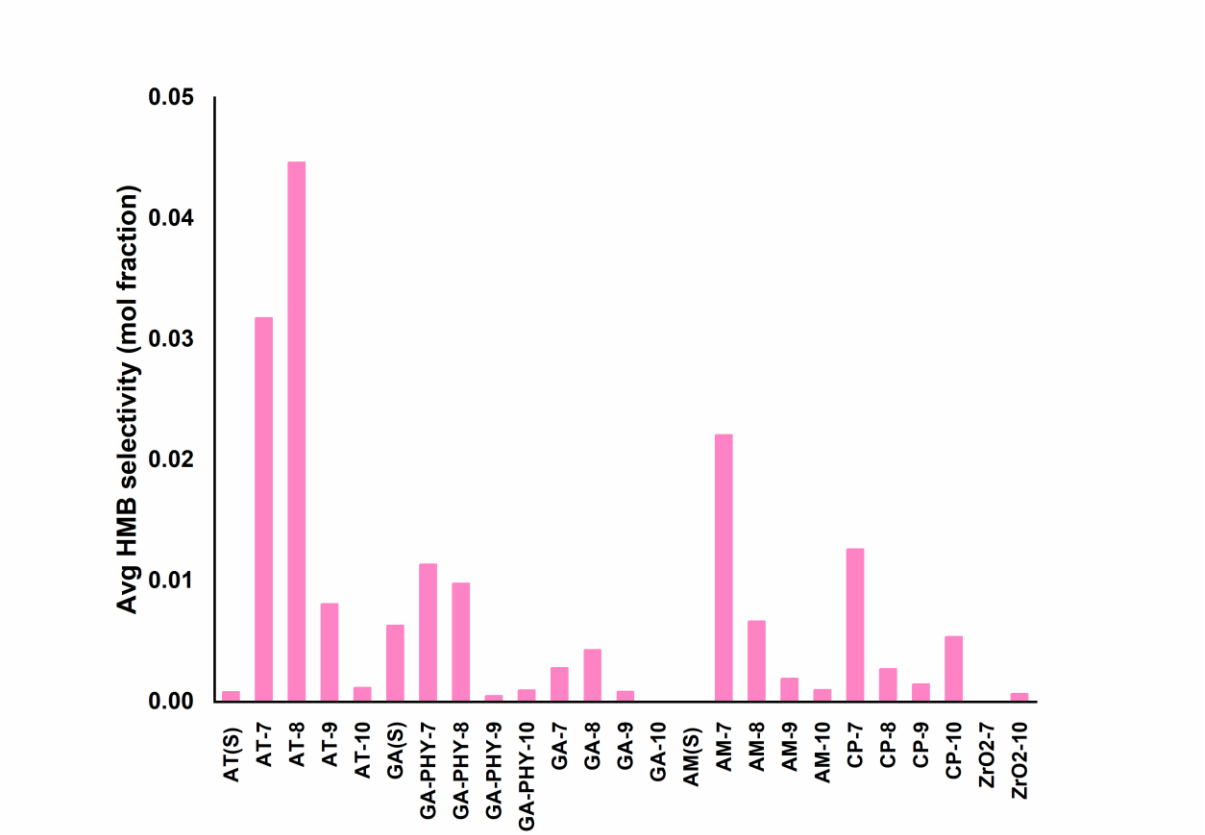

Figure 2. 30: Trends of selectivity for formation of HMB

Since the neat substrates AT(S), AM(S) and GA(S) show lower selectivity to HMB than their bicomponent analogs prepared at pH 7-8, the source of amphoteric character is attributed to zirconia.

Trends for the formation of MiPk are shown in Figure 2.31.

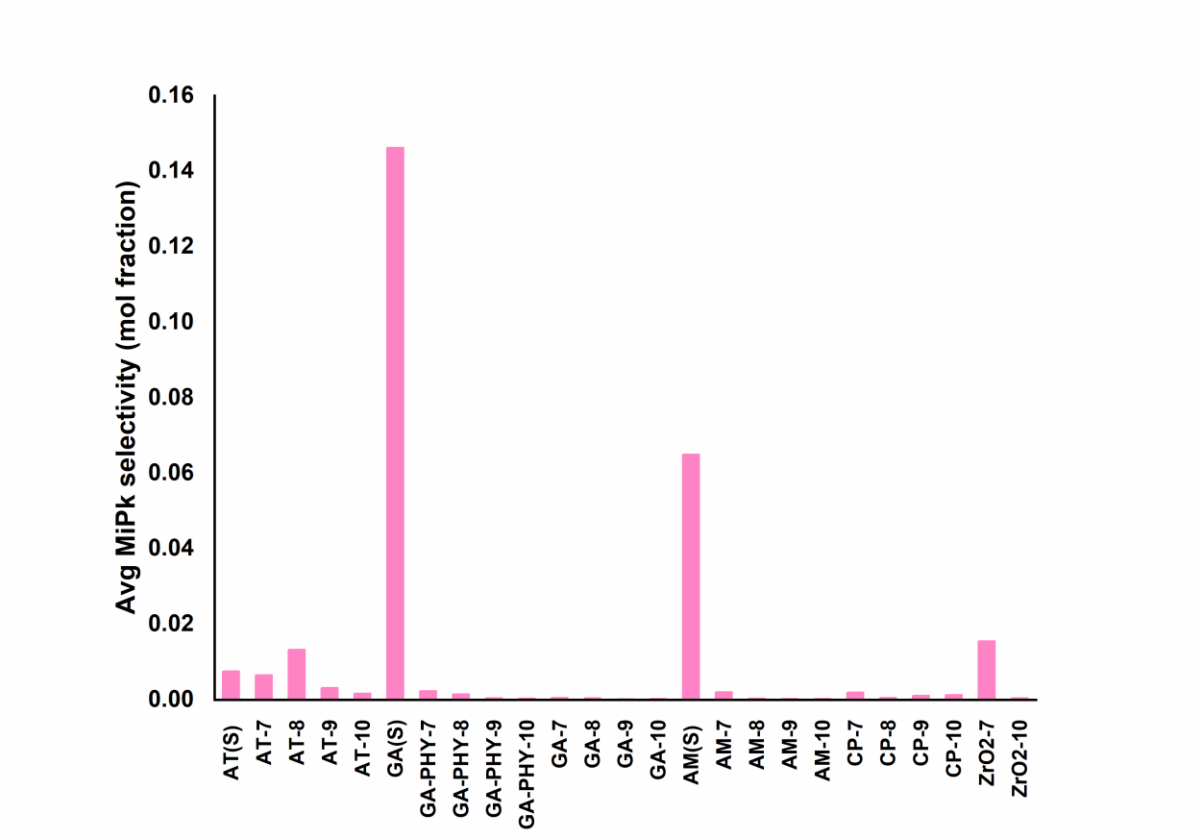

Figure 2. 31: Trend of selectivity for formation of MiPk

Selectivity of these materials to MiPk are AT (S) = 1.1 mol%, ZrO2-7 = 2.0 mol%), ZrO_2-10 = 0.03%, AM (S) = 8.4 mol% and GA(S) = 14.0 mol%. This trend is in the same ascending order as that of the formation of MByne over these materials.

Samples precipitated at pH 7 and 8 show relatively higher selectivity to MiPk than samples prepared at pH 9 or 10. Trends of formation of MiPk for the bi-component series of supports are similar to those of HMB. A possible reason could be because MiPk is reported to form through dehydration of HMB[31]. The trends are also similar to those of MByne.

2.5.5 Stability of the supports

The method of calculating activity is explained in preceding sections (section 2.3 above).

The activity and time on stream data were fitted to a power law equation to obtain the deactivation rate constant using the equation mentioned below (equation 8).

$$A = C \times t^{kd}$$ Equation 8

Decay constants which was determined from above equation are plotted for the different supports as value of exponent of power function in Figure 2.32.

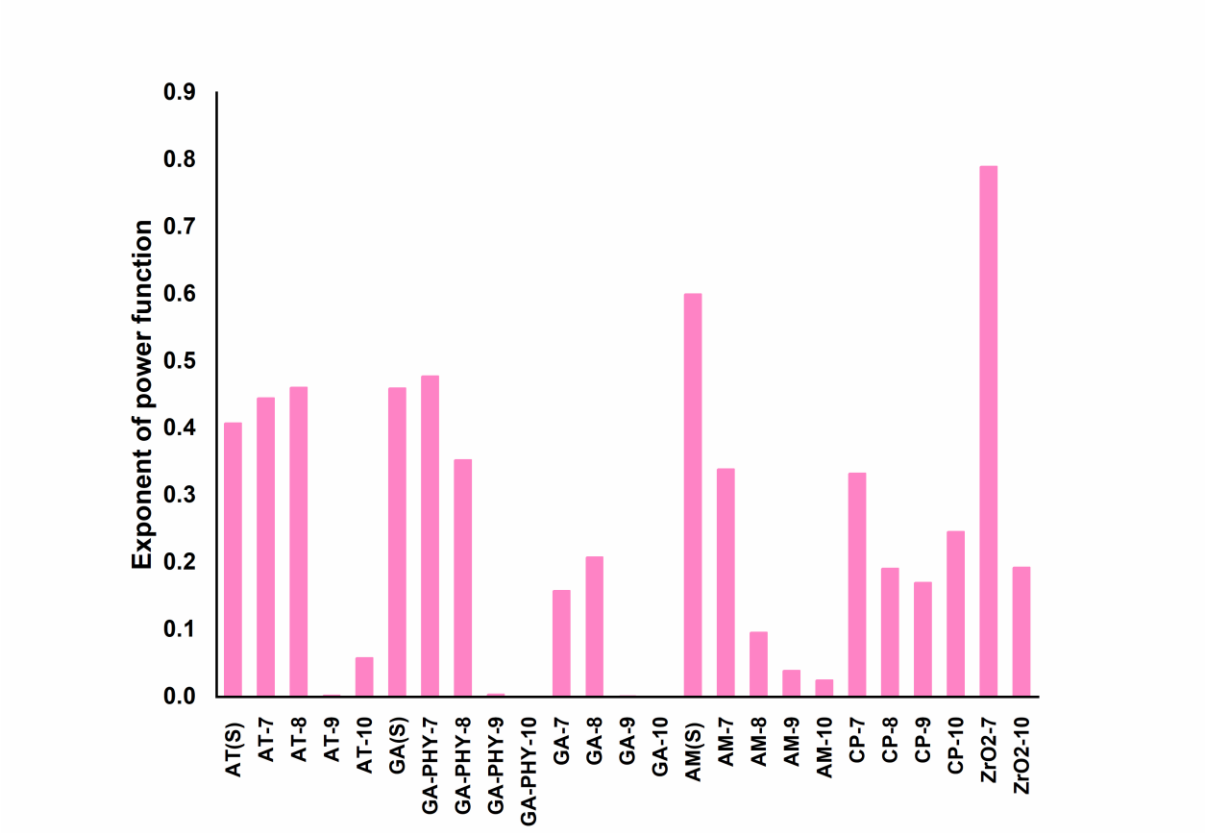

Figure 2. 32: Comparison of decay constants for reaction of MBOH

It is seen from Figure 2.32 that, amongst the mono-component materials, ZrO_2-7 deactivates fastest followed by AM(S), GA(S), AT(S) and lastly ZrO_2-10. (ZrO_2-7>>AM(S)>GA(S)>AT(S)>ZrO_2-10).

For a given series of supports which are prepared by deposition-precipitation, support samples prepared at pH 9 or 10 have significantly higher stability (smaller decay constants) than those prepared at pH 7 or 8. This is true even for neat zirconia samples (ZrO_2-7 deactivates much

faster than ZrO_2-10). It is notable that specific surface area and pore volume of supports prepared at pH ≤8 are significantly higher than those prepared at pH >8 yet they deactivate faster.

It is interesting to note that the decay constants of the samples of bi-component supports GA-9 (decay constant $1.00*10^{-3}$) and GA-10 (decay constant $5.00*10^{-4}$) which were prepared at pH 9 and 10 respectively, are at least 2 orders of magnitude lower than that of the remaining samples, which include sample of neat zirconia prepared at pH 10 (ZrO_2-10). They exhibit synergy because the decay constants are significantly smaller than those of individual γ-Al_2O_3 and ZrO_2 supports.

The CP supports which are prepared by coprecipitation do not show this advantage at higher pH.

The color of catalysts which presented deactivation in the present work was between brown to dark brown after reaction of MBOH. Initial color was white to off-white.

There is no relation between value of decay constant and specific surface area of the five series of supports, however between the alumina substrates deactivation decreases with decreasing specific surface area. From an acid-base standpoint AT(S) which is most basic deactivates at a lower rate than the other two substrates. The more amphoteric AM(S) deactivates faster than GA(S). It is however clear that chemical moiety matters. Amongst the monocomponent supports viz, the three alumina substrates and neat zirconia, AT(S), ZrO_2-7 and ZrO_2-10 show predominantly basic character whereas AM(S) and GA(S) show acidic / amphoteric character. Lauron-Pernot[62] has reviewed the literature on the evaluation of acidic-basic properties of inorganic oxides using model catalytic alcohol reactions. She has reviewed and cited spectroscopic studies during the reaction of MBOH to explain deactivation. On acidic catalysts such as H-ZSM-5 and alkali exchanged H-ZSM-5 Huang and Kaliaguine[63] have carried out IR spectroscopic studies and shown the formation of polyaromatic hydrocarbons or coke. Aramendia et al.[64] have carried out mass spectrometry studies on basic or amphoteric catalysts which show condensation-polymerization of acetone.

Aramendia et.al.[64] have compared deactivation of ZrO_2 and MgO for this reaction. They report that MgO which is more basic than ZrO_2 does not present deactivation behavior, whereas ZrO_2 which is amphoteric in character shows high initial deactivation. The results of the current study are in agreement with those reported by Aramendia et.al. in that samples which present basic

character show significantly slower deactivation. Kaliaguine and Huang[63] have also reported similar behavior in their work. These authors reason that a combination of sufficiently strong Lewis basicity and Lewis acidity is required for the condensation of acetone, the product of which brings about deactivation. An alternate cause for deactivation in the case of catalysts which are strongly acidic is the strong adsorption of MBOH which results in laydown of coke. It is also interesting that supports prepared at pH≤ 8 (in the current study) have specific surface area which is double than those of supports which are prepared at pH > 8. However, the latter, (in spite of lower surface area) present significantly slower deactivation. As seen from results of CHN analysis, Zirconium forms higher amounts of its carbonate than its hydroxide as pH of precipitation increases (Table 2.5). Further, FTIR studies (Figure 2.16 and 2.17) show that the metal carbonate (of zirconium) also changes its form as pH of precipitation is increased. Thus, chemical moiety appears to have a stronger influence in stability of catalysts for reaction of MBOH than physical properties such as specific surface area. It is also noted that the samples of the monocomponent ZrO_2 series deactivate faster than their corresponding bi-component zirconia-alumina supports. This is attributed to their higher acidity as observed from higher selectivity to Mbyne. Thus, the bi-component supports present synergy between zirconia and γ-alumina, which manifests in the form of higher stability in the conversion of MBOH.

Based on the above results deposition-precipitation of zirconia onto the γ-Al2O3 substrate is deemed suitable for further studies wherein Co, Ni and Cu supported on zirconia-alumina would be evaluated for transformation of styrene oxide and for HDO (hydrodeoxygenation) of m-cresol. This combination provides good textural properties and means to vary acid-base properties through their composition. Acidity and basicity influence the formation of 2-PEA and PAA respectively from styrene oxide. Similarly, acid base properties are reported to influence product distribution in HDO of m-cresol. A set of bi-component zirconia-γ-alumina supports with varying zirconia:alumina molar ratios was prepared at pH 9 and used for preparing supported metal catalysts for evaluation in the above mentioned reactions. The details are covered in chapters 3-5.

2.6 Conclusions

As observed from the results of the above studies, deposition-precipitation (DP) is a simple method of preparation which is useful for improving poor textural properties of some materials such as zirconia. Three different alumina based substrates with widely varying properties were

studied. The γ-alumina substrate lends its microstructure to the bi-component system therein dispersing zirconia. XRD studies indicated strong interaction between zirconia and alumina substrates which retarded crystallization of zirconia. This also reflected in very good activity and stability in the decomposition of MBOH. Stability was better than individual γ-alumina and zirconia components. Thus, this substrate shows good synergy with zirconia.

The AM (pseudoboehmite) substrate resulted in significant loss of microstructure in the bicomponent supports. This is attributed to ease of its peptization under the conditions of preparation. XRD shows segregation of zirconia at higher pH of preparation. Thus it is not a good substrate for deposition-precipitation.

The AT (aluminum trihydrate) substrate also showed poor microstructure due to low geometric surface area which hindered the dispersion of zirconia. This reflected in its activity for decomposition of MBOH. Thus it too is not suitable as a substrate for deposition-precipitation.

Coprecipitation resulted in poor microstructure of the bicomponent supports when compared to the GA series (prepared by deposition-precipitation). The former shows poor performance for decomposition of MBOH. XRD shows segregation of zirconia at higher pH of preparation.

Overall, the γ-Al_2O_3 substrate presented advantages of inhibiting sintering of zirconia and also good specific surface area, pore volume and pore diameter. Thus deposition-precipitation using γ-Al_2O_3 substrate appears to be a good method for the preparation of bicomponent zirconia-alumina supports.

pH of preparation had a profound effect on microstructure, XRD crystallite size, type of metal-carbonate and the ratio of carbonate:hydroxide of zirconia in as synthesized supports.

DSC-TG studies also indicated clear differences in interaction between zirconia and these substrates and also catalysts prepared by co-precipitation. TGA-MS identified presence of different species of metal-carbonates and occluded nitrate, whereas FTIR studies identified the dependence of structure of metal-carbonates with pH of preparation. Combining results of CHN and ICP-OES helped to identify changes in carbonate and hydroxide of zirconia with pH of preparation and determine generic composition of the as-synthesized bicomponent supports.

Thus, the method of deposition-precipitation is advantageous in preparation of bi-component supports when one of the components (zirconia in this specific case) tends to have a low surface area. However, higher pH (>9) forms gel-like precipitate of zirconia which limits this

advantage. It causes pore blockage and occlusion of impurities such as sodium nitrate in the supports which is undesirable. However, deposition-precipitation eases the removal of the sodium nitrate by enhanced washing.

The learning from these studies were leveraged to prepare additional set of zirconia-alumina bicomponent supports which were used for preparing bifunctional supported metal catalysts of Co, Ni and Cu (Chapter 3). These catalysts were evaluated for the transformation of styrene oxide (Chapter 4) and hydrodeoxygenation of m-cresol (Chapter 5).

2.7 References

[1] R. P. Sunil K Kanojiya, Arvind Patel, Gaurav Shukla, Neerja Joshi, Prabhakar Sharma P L Gupta, M Batra, "Hydrogenation of styrene oxide to 2-phenyl ethanol over supported Nanonickel catalyst," *Int. J. Sci. Eng. Res.*, vol. 6, no. 2, 2015.

[2] F. Zaccheria, R. Psaro, N. Ravasio, L. Sordelli, and F. Santoro, "Mono and bifunctional catalysts for styrene oxide isomerization or hydrogenation," *Catal. Letters*, vol. 141, no. 4, pp. 587–591, 2011, doi: 10.1007/s10562-010-0543-5.

[3] D. Poondi and M. A. Vannice, "The influence of MSI (metal-support interactions) on phenylacetaldehyde hydrogenation over Pt catalysts," *J. Mol. Catal. A Chem.*, vol. 124, no. 1, pp. 79–89, Sep. 1997, doi: 10.1016/S1381-1169(97)00066-6.

[4] H. Kochkar, J. M. Clacens, and F. Figueras, "Isomerization of styrene epoxide on basic solids," *Catal. Letters*, vol. 78, no. 1–4, pp. 91–94, 2002, doi: 10.1023/A:1014914207019.

[5] A. Sasu, B. Dragoi, A. Ungureanu, S. Royer, E. Dumitriu, and V. Hulea, "Selective conversion of styrene oxide to 2-phenylethanol in cascade reactions over non-noble metal catalysts," *Catal. Sci. Technol.*, vol. 6, no. 2, pp. 468–478, 2016, doi: 10.1039/C5CY00779H.

[6] F. Hoelderich, Wollfgang, W. Norbert Goetz, and F. Leopold Hupfer, "Preparation of phenylethanols," US 4943667, 1990.

[7] M. L. Gou, R. Wang, Q. Qiao, and X. Yang, "Effect of phosphorus on acidity and performance of HZSM-5 for the isomerization of styrene oxide to phenylacetaldehyde,"

Appl. Catal. A Gen., vol. 482, pp. 1–7, 2014, doi: 10.1016/j.apcata.2014.05.023.

[8] M.-L. Gou, R. Wang, Q. Qiao, and X. Yang, "Effect of mesoporosity by desilication on acidity and performance of HZSM-5 in the isomerization of styrene oxide to phenylacetaldehyde," *Microporous Mesoporous Mater.*, vol. 206, pp. 170–176, Apr. 2015, doi: 10.1016/j.micromeso.2014.12.006.

[9] I. Kirm, F. Medina, X. Rodríguez, Y. Cesteros, P. Salagre, and J. E. Sueiras, "Preparation of 2-phenylethanol by catalytic selective hydrogenation of styrene oxide using palladium catalysts," *J. Mol. Catal. A Chem.*, vol. 239, no. 1–2, pp. 215–221, 2005, doi: 10.1016/j.molcata.2005.06.032.

[10] H. C. Bajaj, S. Hasan, R. Abdi, R. I. Kureshy, N. H. Khan, and A. Asharafbhai, "Hydrogenation of styrene oxide forming 2-phenyl ethanol," US 9040755 B2, 2015.

[11] O. Bergadà, P. Salagre, Y. Cesteros, F. Medina, and J. E. Sueiras, "Control of the basicity in Ni-MgO systems: Influence in the hydrogenation of styrene oxide," *Catal. Letters*, vol. 122, no. 3–4, pp. 259–266, 2008, doi: 10.1007/s10562-007-9373-5.

[12] P. Mäki-Arvela and D. Murzin, "Hydrodeoxygenation of Lignin-Derived Phenols: From Fundamental Studies towards Industrial Applications," *Catalysts*, vol. 7, no. 9, p. 265, Sep. 2017, doi: 10.3390/catal7090265.

[13] P. M. Mortensen, J.-D. Grunwaldt, P. A. Jensen, and A. D. Jensen, "Screening of Catalysts for Hydrodeoxygenation of Phenol as a Model Compound for Bio-oil," *ACS Catal.*, vol. 3, no. 8, pp. 1774–1785, Aug. 2013, doi: 10.1021/cs400266e.

[14] I. T. Ghampson *et al.*, "Phenol hydrodeoxygenation: effect of support and Re promoter on the reactivity of Co catalysts," *Catal. Sci. Technol.*, vol. 6, no. 19, pp. 7289–7306, 2016, doi: 10.1039/C6CY01038E.

[15] M. M. Ambursa *et al.*, "Equity Journal of Science and Technology , 2020 7 (2): 136 - 143 An Official Publication of Kebbi State University of Science and Technology , Aliero , Nigeria A Review on Required Catalysts Composition and its Effective Preparation Method for Hydrodeox," vol. 7, no. 2, pp. 136–143, 2020.

[16] R. Agustin-Panadero, J. Roman-Rodriguez, A. Ferreiroa, M. Sola-Ruiz, and A. Fons-Font,

"Zirconia in fixed prosthesis. A literature review," *J. Clin. Exp. Dent.*, pp. e66-73, 2014, doi: 10.4317/jced.51304.

[17] Michel Deeba, T. Luo, and J. Ramos, "Palladium-supported catalyst composites," US 8568675 B2, 2013.

[18] S. M. Ulfa, K. A. Putra, and M. F. Rahman, "Influence of Ni loading on hydrodeoxygenation of phenol using Ni/Al2O3-ZrO2 catalyst by flow reactor system," 2018, p. 050012, doi: 10.1063/1.5062762.

[19] C. A. Teles, R. C. Rabelo-Neto, J. R. de Lima, L. V. Mattos, D. E. Resasco, and F. B. Noronha, "The Effect of Metal Type on Hydrodeoxygenation of Phenol Over Silica Supported Catalysts," *Catal. Letters*, vol. 146, no. 10, pp. 1848–1857, Oct. 2016, doi: 10.1007/s10562-016-1815-5.

[20] C. A. Teles, R. C. Rabelo-Neto, G. Jacobs, B. H. Davis, D. E. Resasco, and F. B. Noronha, "Hydrodeoxygenation of Phenol over Zirconia-Supported Catalysts: The Effect of Metal Type on Reaction Mechanism and Catalyst Deactivation," *ChemCatChem*, vol. 9, no. 14, pp. 2850–2863, Jul. 2017, doi: 10.1002/cctc.201700047.

[21] N. M. Deraz, "The comparative jurisprudence of catalysts preparation methods : II . Deposition-precipitation and adsorption methods .," vol. 2, no. 2, pp. 1–3, 2018.

[22] L. Zhang, G. Wen, H. Liu, N. Wang, and D. S. Su, "Preparation of Palladium Catalysts Supported on Carbon Nanotubes by an Electrostatic Adsorption Method," *ChemCatChem*, vol. 6, no. 9, pp. 2600–2606, 2014, doi: https://doi.org/10.1002/cctc.201402175.

[23] C. Perego and P. Villa, "Catalyst preparation methods," *Catal. Today*, vol. 34, no. 3–4, pp. 281–305, 1997, doi: https://doi.org/10.1016/S0920-5861(96)00055-7.

[24] L. S. Roselin, F. Chang, W. Chen, and H. Yang, "A Comparison Between Deposition–Precipitation and Co-Precipitation Methods for the Preparation of Au–Ru/Fe2O3 Nanostructure Catalysts Tested for Partial Oxidation of Methanol," *Sci. Adv. Mater.*, vol. 3, no. 6, pp. 893–900, 2011, doi: https://doi.org/10.1166/sam.2011.1214.

[25] J. A. Wang, M. A. Valenzuela, J. Salmones, A. Vázquez, A. García-Ruiz, and X. Bokhimi, "Comparative study of nanocrystalline zirconia prepared by precipitation and sol–gel

methods," *Catal. Today*, vol. 68, no. 1–3, pp. 21–30, Jul. 2001, doi: 10.1016/S0920-5861(01)00319-4.

[26] T. I. Panova, L. V. Morozova, and I. G. Polyakova, "Synthesis and investigation of properties of nanocrystalline zirconia and hafnia," *Glas. Phys. Chem.*, vol. 37, no. 2, pp. 179–187, Apr. 2011, doi: 10.1134/S1087659611020118.

[27] I. A. Stenina, E. Y. Voropaeva, A. G. Veresov, G. I. Kapustin, and A. B. Yaroslavtsev, "Effect of Precipitation pH and Heat Treatment on the Properties of Hydrous Zirconium Dioxide," *Russ. J. Inorg. Chem.*, vol. 53, no. 3, pp. 350–356, Mar. 2008, doi: 10.1134/S0036023608030029.

[28] B. H. Davis, "Effect of pH on Crystal Phase of ZrO2 Precipitated from Solution and Calcined at 600°C," *J. Am. Ceram. Soc.*, vol. 67, no. 8, p. C-168, 1984, doi: 10.1111/j.1151-2916.1984.tb19185.x.

[29] O. Y. Kurapova and V. G. Konakov, "Phase evolution in zirconia based systems," *Rev. Adv. Mater. Sci.*, vol. 36, no. 2, pp. 177–190, 2014.

[30] W. Stichert and F. Schüth, "Influence of Crystallite Size on the Properties of Zirconia," *Chem. Mater.*, vol. 10, no. 7, pp. 2020–2026, Jul. 1998, doi: 10.1021/cm980705o.

[31] H.Lauron-Pernot, F.Luck, and J.M.Popa, "Methylbutynol: a new and simple diagnostic tool for acidic and basic sites of solids," *Appl. Catal.*, vol. 78, no. 2, pp. 213–225, 1991, doi: https://doi.org/10.1016/0166-9834(91)80107-8.

[32] T. T. W. Hummel, U. Berner, E. Curti,F.J. Pearson, "nagra, TECHNICALREPORT 02 - 16."

[33] S. O. Mc Arthur, Mary J, "No Title," European patemt specification Publication number 0 004 403 B1, 1969.

[34] Z. Pospelova, "No Title," *Russ. J. Inorg. Chem.*, vol. 2, no. 8, pp. 995–1004, 1966.

[35] Raymond J. Wong, "Sodium zirconium carbonate and zirconium basic carbonate and methods of making the same," US6627164B1, 2003.

[36] Z. Feng, W. S. Postula, A. Akgerman, and R. G. Anthony, "Characterization of Zirconia-

Based Catalysts Prepared by Precipitation, Calcination, and Modified Sol-Gel Methods," *Ind. Eng. Chem. Res.*, vol. 34, no. 1, pp. 78–82, Jan. 1995, doi: 10.1021/ie00040a005.

[37] K. Wefers and C. Misra, "Oxides and Hydroxides of Aluminum," *Alcoa Tech. Pap.*, vol. 19, pp. 1–100, 1987.

[38] X. L. Zhou *et al.*, "On the Role of Calcination Temperature in Pt-SO 4 2− /ZrO2−Al2O3 Preparation and Catalytic Behaviors During the n-Hexane Hydroisomerization," *Catal. Letters*, vol. 124, no. 3–4, pp. 277–283, Aug. 2008, doi: 10.1007/s10562-008-9449-x.

[39] C. Huang, Z. Tang, and Z. Zhang, "Differences between Zirconium Hydroxide (Zr(OH)4 nH2O) and," *J. Am. Ceram. Soc.*, vol. 84, no. 7, pp. 1637–1638, 2001.

[40] C. Huang, Z. Tang, Z. Zhang, and J. Gong, "Study on a new, environmentally benign method and its feasibility of preparing nanometer zirconia powder," *Mater. Res. Bull.*, vol. 35, no. 9, pp. 1503–1508, 2000, doi: 10.1016/S0025-5408(00)00349-4.

[41] C. J. Serna, J. L. White, and S. L. Hem, "Nature of Amorphous Aluminum Hydroxycarbonate," *J. Pharm. Sci.*, vol. 67, no. 8, pp. 1144–1147, Aug. 1978, doi: 10.1002/jps.2600670831.

[42] C Jeffrery Brinker ; and Scherrer George W, *sol-gel science:the physics and chemistry of sol-gel processing*. San diago: Acadamic press, Elsivier, 1990.

[43] B. Torres-olea, M. Sandra, C. Garc, J. A. Cecilia, and P. Maireles-torres, "Glucose conversion into 5-hydroxymethylfurfural," *Catalysts*, vol. 10, no. 878, pp. 1–21, 2020.

[44] E. Rubio, V. Rodriguez-Lugo, R. Rodriguez, and V. M. Castano, "Nano zirconia and sulfated zirconia from ammonia zirconium carbonate," *Rev. Adv. Mater. Sci.*, vol. 22, no. 1–2, pp. 67–73, 2009.

[45] D. L. D. Laing, T. Bauer, W.-D. Steinmann, "ADVANCED HIGH TEMPERATURE LATENT HEAT STORAGE SYSTEM – DESIGN AND TEST RESULTS," in *The 11th International Conference on Thermal Energy Storage – Effstock 14-17 June 2009 in Stockholm, Sweden*, 2009, no. June, pp. 1–8.

[46] H. Li *et al.*, "Synthesis of glycerol carbonate by direct carbonylation of glycerol with CO 2

over solid catalysts derived from Zn/Al/La and Zn/Al/La/M (M = Li, Mg and Zr) hydrotalcites," *Catal. Sci. Technol.*, vol. 5, no. 2, pp. 989–1005, 2015, doi: 10.1039/C4CY01237B.

[47] S. Kouva, J. Andersin, K. Honkala, J. Lehtonen, L. Lefferts, and J. Kanervo, "Water and carbon oxides on monoclinic zirconia: experimental and computational insights," *Phys. Chem. Chem. Phys.*, vol. 16, no. 38, pp. 20650–20664, 2014, doi: 10.1039/C4CP02742F.

[48] M. J. M. A. L. B. M. A. L. Scarbrough, "A sodium zirconium carbonate compound and the method of its preparation," EP0004403B1, 1981.

[49] P. Examiner and M. L. Shippen, "Process for the preparation of 2-phenyl ethanol," US 6166269, 2000.

[50] V. Santos, M. Zeni, C. P. Bergmann, and J. M. Hohemberger, "Correlation between thermal treatment and tetragonal/monoclinic nanostructured zirconia powder obtained by sol-gel process," *Rev. Adv. Mater. Sci.*, vol. 17, no. 1–2, pp. 62–70, 2008.

[51] B.G.linsen, Ed., "Chapter-1," in *Physical and Chemical Aspects of Adsorbents and Catalysts*, Acadamic press, London and New York, 1970, pp. 1–59.

[52] B. L. Kirsch and S. H. Tolbert, "Stabilization of Isolated Hydrous Amorphous and Tetragonal Zirconia Nanoparticles Through the Formation of a Passivating Alumina Shell," *Adv. Funct. Mater.*, vol. 13, no. 4, pp. 281–288, 2003, doi: http://dx.doi.org/10.1002/adfm.200304267.

[53] A. Morikawa, T. Suzuki, T. Kanazawa, K. Kikuta, A. Suda, and H. Shinjo, "A new concept in high performance ceria–zirconia oxygen storage capacity material with Al2O3 as a diffusion barrier," *Appl. Catal. B Environ.*, vol. 78, no. 3, pp. 210–221, 2008, doi: http://dx.doi.org/10.1016/j.apcatb.2007.09.013.

[54] S. Shukla and S. Seal, "Mechanisms of room temperature metastable tetragonal phase stabilisation in zirconia," *Int. Mater. Rev.*, vol. 50, no. 1, pp. 45–64, Feb. 2005, doi: 10.1179/174328005X14267.

[55] R. A. Sigwadi, S. E. Mavundla, N. Moloto, and T. Mokrani, "Synthesis of zirconia-based solid acid nanoparticles for fuel cell application," *J. Energy South. Africa*, vol. 27, no. 2, p.

60, Jul. 2016, doi: 10.17159/2413-3051/2016/v27i2a1342.

[56] A. Adamski, P. Jakubus, and Z. Sojka, “Synthesis of nanostructured tetragonal ZrO2 of enhanced thermal stability,” *Nukleonika*, vol. 51, no. SUPPL. 1, pp. 27–33, 2006.

[57] J. Chevalier, L. Gremillard, A. V. Virkar, and D. R. Clarke, “The Tetragonal-Monoclinic Transformation in Zirconia: Lessons Learned and Future Trends,” *J. Am. Ceram. Soc.*, vol. 92, no. 9, pp. 1901–1920, Sep. 2009, doi: 10.1111/j.1551-2916.2009.03278.x.

[58] G. A. Carter, M. Rowles, M. I. Ogden, R. D. Hart, and C. E. Buckley, “Industrial precipitation of zirconyl chloride: The effect of pH and solution concentration on calcination of zirconia,” *Mater. Chem. Phys.*, vol. 116, no. 2–3, pp. 607–614, Aug. 2009, doi: 10.1016/j.matchemphys.2009.05.014.

[59] H. Lauron-Pernot, F. Luck, and J. M. Popa, “Methylbutynol: a new and simple diagnostic tool for acidic and basic sites of solids,” *Appl. Catal.*, vol. 78, no. 2, pp. 213–225, Nov. 1991, doi: 10.1016/0166-9834(91)80107-8.

[60] K. TOMISHIGE, Y. IKEDA, T. SAKAIHORI, and K. FUJIMOTO, “Catalytic properties and structure of zirconia catalysts for direct synthesis of dimethyl carbonate from methanol and carbon dioxide,” *J. Catal.*, vol. 192, no. 2, pp. 355–362, Jun. 2000, doi: 10.1006/jcat.2000.2854.

[61] C. Lahousse, A. Aboulayt, F. Maugé, J. Bachelier, and J. C. Lavalley, “Acidic and basic properties of zirconia—alumina and zirconia—titania mixed oxides,” *J. Mol. Catal.*, vol. 84, no. 3, pp. 283–297, Oct. 1993, doi: 10.1016/0304-5102(93)85061-W.

[62] H. Lauron-Pernot, “Evaluation of Surface Acido-Basic Properties of Inorganic-Based Solids by Model Catalytic Alcohol Reaction Networks,” *Catal. Rev.*, vol. 48, no. 3, pp. 315–361, Sep. 2006, doi: 10.1080/01614940600816634.

[63] M. Huang and S. Kaliaguine, “Reactions of methylbutynol on alkali-exchanged zeolites. A Lewis acid-base selectivity study,” *Catal. Letters*, vol. 18, no. 4, pp. 373–389, 1993, doi: 10.1007/BF00765284.

[64] M. . Aramendía *et al.*, “Comparison of different organic test reactions over acid–base catalysts,” *Appl. Catal. A Gen.*, vol. 184, no. 1, pp. 115–125, Aug. 1999, doi:

10.1016/S0926-860X(99)00096-4.